RESEARCH ARTICLE

An oxidation-resistant peptide mimic of surfactant protein B (B-YL) forms an amphipathic helix-hairpin in liposomes with high surface activity [version 1; peer review: 1 approved with reservations, 1 not approved]

Frans J. Walther, Monik Gupta, Larry M. Gordon, Alan J. Waring

Department of Pediatrics, Los Angeles Biomedical Research Institute at Harbor-UCLA Medical Center, Torrance, CA, 90502, USA

v1 **First published:** 26 Feb 2018, **2**:13
https://doi.org/10.12688/gatesopenres.12799.1
Latest published: 10 Jul 2018, **2**:13
https://doi.org/10.12688/gatesopenres.12799.2

Abstract

Background: Animal-derived surfactants containing surfactant proteins B (SP-B) and C (SP-C) are used to treat respiratory distress syndrome (RDS) in preterm infants. SP-B (79 residues) plays a pivotal role in lung function and the design of synthetic lung surfactant. Super Mini-B (SMB), a 41-residue peptide based on the N- and C-domains of SP-B joined with a turn and two disulfides, folds as an α-helix hairpin mimicking the properties of these domains in SP-B. Here, we studied 'B-YL', a 41-residue oxidation-resistant SMB variant that has its four Cys and two Met residues replaced by Tyr and Leu, respectively, to test whether these hydrophobic substitutions produce a surface-active, α-helix hairpin.

Methods: Structure and function of B-YL and SMB in surfactant lipids were compared with CD and FTIR spectroscopy and molecular dynamic (MD) simulations, and surface activity with captive bubble surfactometry and in lavaged, surfactant-deficient adult rabbits.

Results: CD and FTIR spectroscopy of B-YL in surfactant lipids showed secondary structures compatible with peptide folding as an α-helix hairpin, similar to SMB in lipids. MD simulations confirmed that B-YL maintained its α-helix hairpin in a lipid bilayer, matching the hairpin obtained from MD of SMB. Unlike the disulfide-reinforced helix-turn of SMB, the B-YL fold was stabilized by a core of clustered Tyr linking the N- and C-helices through noncovalent interactions involving aromatic rings. B-YL in surfactant lipids demonstrated excellent *in vitro* surface activity and good oxygenation and dynamic compliance in lavaged, surfactant-deficient adult rabbits.

Conclusions: 'Sulfur-free' and 'oxidation-resistant' B-YL forms an amphipathic helix-hairpin in surfactant liposomes with high surface activity and is functionally similar to SMB and native SP-B. B-YL's resistance against free oxygen radical damage provides an extra edge over oxidized SMB in the treatment of respiratory failure in preterm

Open Peer Review

Approval Status ✓ ✓

	1	2
version 2 (revision) 10 Jul 2018	✓ view	✓ view
version 1 26 Feb 2018	✗ view	? view

1. **Valerie Booth**, Memorial University of Newfoundland, St. John's, Canada

2. **Jesús Pérez-Gil**, Complutense University, Madrid, Spain

Any reports and responses or comments on the article can be found at the end of the article.

infants with RDS and children and adults with acute lung injury.

Keywords
Surfactant, synthetic lung surfactant, surfactant protein B, SP-B peptide mimic, surface activity, oxidation resistance, respiratory distress syndrome, acute respiratory distress syndrome

Corresponding author: Frans J. Walther (fwalther@labiomed.org)

Author roles: Walther FJ: Conceptualization, Funding Acquisition, Investigation, Methodology, Project Administration, Resources, Supervision, Writing – Original Draft Preparation, Writing – Review & Editing; **Gupta M**: Formal Analysis, Investigation; **Gordon LM**: Conceptualization, Formal Analysis, Investigation, Methodology, Writing – Original Draft Preparation; **Waring AJ**: Conceptualization, Formal Analysis, Investigation, Methodology, Validation, Writing – Review & Editing

Competing interests: No competing interests were disclosed.

Grant information: Bill and Melinda Gates Foundation [OPP1112090].
The funders had no role in study design, data collection and analysis, decision to publish, or preparation of the manuscript.

How to cite this article: Walther FJ, Gupta M, Gordon LM and Waring AJ. **An oxidation-resistant peptide mimic of surfactant protein B (B-YL) forms an amphipathic helix-hairpin in liposomes with high surface activity [version 1; peer review: 1 approved with reservations, 1 not approved]** Gates Open Research 2018, **2**:13 https://doi.org/10.12688/gatesopenres.12799.1

First published: 26 Feb 2018, **2**:13 https://doi.org/10.12688/gatesopenres.12799.1

Introduction

Lung surfactant is a lipid-protein mixture that is synthesized by alveolar type II cells and secreted into the alveolus where it reduces surface tension at the air-liquid interface. Mammalian lung surfactant harvested by lavage consists of approximately 80% phospholipids, 10% neutral lipids and 10% protein[1]. Phosphatidylcholine (PC), and particularly dipalmitoylphosphatidylcholine (DPPC), is the major phospholipid constituent of lung surfactant. DPPC enhances the formation of a rigid film at the air-liquid interface that reduces alveolar surface tension to low values during dynamic compression, whereas fluid phospholipids and neutral lipids are important because they significantly improve film spreading[2,3]. The highly hydrophobic surfactant protein B (SP-B) and, to a lesser extent, surfactant protein C (SP-C), facilitate the absorption of phospholipids into the air-liquid interface and thus play an important role in the reduction of alveolar surface tension. SP-B is pivotal for normal lung function, by hereditary SP-B deficiency being fatal in newborn infants[4] and also in SP-B knockout mice[5]. Human SP-B is a 79 amino-acid, lipid-associating monomer (MW ~8.7 kDa) found in the lung as a covalently linked homodimer. Early theoretical studies based on homology comparisons indicated that the SP-B monomer consists of 4-5 α-helices[6–10] with three intramolecular disulfide bridges (i.e., Cys-8 to Cys-77, Cys-11 to Cys-71 and Cys-35 to Cys-46)[11], and belongs to the saposin protein superfamily[12]. The helical bundle for SP-B folds into two leaves, with one leaf having α-helices 1 (N-terminal helix), 5 (C-terminal helix) and 4 and the other composed of α-helices 2 and 3[13,14].

Intratracheal administration of animal-derived lung surfactants, which contain only polar lipids and native SP-B and SP-C, has greatly improved morbidity and mortality of premature infants with neonatal respiratory distress syndrome (RDS) as a result of surfactant-deficiency due to lung immaturity[15]. Existing clinically available formulations are extracted from lung lavages or homogenates from pigs (Curosurf®) and cows (Infasurf®, Survanta®), and contain small amounts of SP-B and SP-C (<< 2% of total weight) in a lipid extract with DPPC as its main component. Based on the predicted 3D-saposin motif for SP-B, we have developed minimal SP-B constructs that have desirable structural properties and maintain high activities in animal models of surfactant deficiencies[9,10]. For example, Super Mini-B (SMB) is a 41-residue, 'short-cut' peptide (Figure 1A), based on the primary sequence, secondary structure and tertiary folding of the known sequence of native SP-B (79-residues), that mimics the high surfactant activity of its parent protein[10,14,16]. SMB incorporates the N-terminal α-helix (~residues 8-25) and C-terminal α-helix (~residues 63-78) of native SP-B as a single linear peptide (Figure 1A), joined together with a customized turn to form a α-helix hairpin. The oxidized SMB in Figure 1A has two vicinal disulfide bonds (i.e., Cys-8 to Cys-77 and Cys-11 to Cys-71) that further covalently link the N- and C-terminal α-helices, and also a hydrophobic N-terminal insertion sequence (i.e., residues 1-7; FPIPLPY). Experimental procedures validated the above structural model for SMB, including conventional ^{12}C-FTIR spectroscopy, mass spectroscopy, I-TASSER homology modeling, and Molecular Dynamics (MD) simulations in lipid mimics and lipid bilayers[14,16,17]. When formulated with a lipid composition that mimics that of native lung surfactant, SMB has shown excellent surface activity with fresh and stored preparations, which was closely associated with the formation of an α-helix hairpin[10,14,17].

Because surfactant therapy is life-saving in preventing and treating RDS in preterm infants, on-going research is studying whether surfactant therapy may be efficaciously extended to pediatric and adult patients with clinical acute lung injury (ALI) or the acute respiratory distress syndrome (ARDS)[18]. ALI and ARDS may each be caused by direct exposure of lungs to pathogens, oxidative air pollutants, cigarette smoke and other irritants in the alveolar space, and by the presence of endogenous reactive oxygen species (ROS) in damaged lungs due to permeability edema or the inflammatory response. Subsequent oxidative alterations may produce dysfunctional and even inactive lung surfactant in these diseases[19,20]. SP-B is an important target for ROS-induced oxidative surfactant inactivation[21,22]. Specifically, oxidation of native SP-B involves alterations in the methionines (Met-29, Met-65) and tryptophan (Trp-9), which correlates well with the loss of *in vitro* surfactant activity[22]. Mimics based on the native SP-B sequence may be likewise sensitive to oxidation processes. Kim *et al.*[23] reported that ozone treatment of SP-B(1–25), an SP-B mimic whose sequence overlaps residues 1–25 of SMB (Figure 1A) and native SP-B, variably oxidized amino-acids known to react with ozone. In contrast to the nearly complete homogenous oxidation of the susceptible SP-B(1–25) residues (i.e., Cys-8, Cys-11, Trp-9, and Met-21) in the solvent phase, only a limited subset of residues (Trp-9 and Met-21) oxidized in the hydrophobic interfacial environment provided by the lipid surfactant layer[23]. In additional studies, Hemming *et al.*[24] showed that exposure of either SP-B$_{1-25}$ or SMB at the air-water interface to dilute ozone (~2 ppm) produced a rapid loss of surface activity (i.e., increase in surface tension). Because decreases in tryptophan fluorescence occurred concurrently with increasing surface tension for these two SP-B mimics[24], it is likely that oxidative disruption of the indole ring of Trp-9 plays a role in the diminished surface activity, possibly due to a fraying of the N-terminal α-helix[24,25].

The development of surfactant therapy for ALI/ARDS is especially challenging as it requires the use of exogenous surfactants that successfully resist inhibition from endogenous ROS in injured lungs. Synthetic lung surfactant with SP-B and SP-C peptide mimics offers substantial advantages over current animal-derived surfactants for treating surfactant deficiency in neonatal RDS and surfactant dysfunction in ALI/ARDS. Current research on synthetic lung surfactant has focused on designing peptide mimics of natural surfactant proteins that are highly effective, stable, and easy to manufacture[9,10]. Here, we conducted structural and functional experiments on 'B-YL' (Figure 1B), a 41-residue SMB variant that has its four Cys and two Met residues replaced by Tyr (Tyr-8, Tyr-11, Tyr-34 and Tyr-40) and Leu (Leu-21 and Leu-28), respectively, and tested whether these

Figure 1. Sequences for oxidized Super Mini-B (SMB) and B-YL. (**A**) SMB (41 amino-acid residues; 1-letter amino-acid notation), with the N- and C-terminal Phe-1 and Ser-41 as indicated, as well as the sulfur-containing cysteines (Cys-8, Cys-11, Cys-34, Cys-40) and methionines (Met-21, Met-28) in red. The disulfide-linkages are shown between Cys-11 and Cys-34 and between Cys-8 and Cys-40. (**B**) B-YL (41 residues) shares the same sequence as its parent SMB, except that the cysteines and methionines are replaced by tyrosines (Tyr-8, Tyr-11, Tyr-34, Tyr-40) and leucines (Leu-21, Leu-28) in red, respectively.

hydrophobic substitutions produce a surface-active, α-helix hairpin.

Methods

Materials

HPLC grade chloroform, methanol, trifluoroethanol (TFE), and acetonitrile were purchased from Fisher Scientific (Pittsburgh, PA 15275), trifluoroacetic acid from Sigma Chemical Co (Saint Louis, MO 63103), NMR quality deuterated water was from Aldrich Chemical Co. (St. Louis, MO 63103), and Sephadex LH-20 chromatography gel from Pharmacia (Uppsala, Sweden). Phospholipids were supplied by Avanti Polar Lipids (Alabaster, AL 35007), and Sodium Dodecyl Sulfate (SDS) detergent was from Sigma Chemical Co (Saint Louis, MO 63103).

The oxidized Super Mini-B (SMB) peptide sequence (Figure 1A) was synthesized using a standard Fmoc protocol with a Symphony Multiple Peptide Synthesizer (Protein Technologies, Inc., Tucson, AZ 87514) or a CEM Liberty microwave synthesizer (CEM Corporation, Mathews, NC 28104), cleaved-deprotected and purified using reverse phase HPLC as described earlier[14,17]. This synthesis protocol included folding of the peptide in a structure-promoting TFE-buffer solvent system to promote oxygen-mediated disulfide linkages between Cys-8 and Cys-40 and between Cys-11 and Cys-34[10,14]. This covalently stabilized connectivity gave the peptide a helix-hairpin conformation, comparable to the topological organization seen for the N- and C-terminal helical domains of the saposin family of proteins[9,10,12]. The synthesis of B-YL was identical to that of SMB, except for replacing cysteines with tyrosines (Tyr-8, Tyr-11, Tyr-34, and Tyr-40) and methionines with leucines (Leu-21 and Leu-28), and also omitting the oxidation step. The purified SMB and B-YL peptides were each freeze-dried directly, and the masses were confirmed by MALDI TOF mass spectrometry as described previously[17].

Preparation of proteins and lipids in surfactant dispersions

Peptide and lipids were formulated as lipid-peptide dispersions to have a total of 2–4% by mole fraction of SMB or B-YL and 35 mg of total lipid [i.e., DPPC: POPC: POPG 5:3:2 mole:mole] per mL of dispersion. The peptide was dissolved in 10 mL of trifluoroethanol and co-solvated with the lipid in chloroform, followed by removal of the solvents with a stream of nitrogen gas and freeze drying of the resulting lipid-peptide film to remove residual solvent. The film was then dispersed with Phosphate Buffered Saline and the sample flask containing the hydrated film was rotated for 1 h at 60°C to produce a solution of multilamellar vesicles (MLVs)[14]. Lipid controls were similarly prepared but without peptide. These dispersions were then stored at 4°C prior to structural and functional measurements. To determine the molecular mass of peptides formulated with lipids, the peptide was separated from lipid using normal phase chromatography with Sephadex LH-20[26].

Circular dichroism (CD) spectroscopy of the secondary structure of the B-YL mimic

CD spectra (190–260 nm) of the B-YL peptide in various structure-promoting environments, including surfactant dispersions, were measured with a JASCO 715 spectropolarimeter (Jasco Inc., Easton MD 21601). The instrument was routinely calibrated for wavelength and optical rotation using 10-camphorsulphonic acid[27]. The sample solutions were scanned using 0.01 cm pathlength cells at a rate of 20 nm per minute, a sample interval of 1 nm, and a temperature of 37°C. Sample concentration was determined by UV absorbance at 280 nm[28]. Peptide concentration was 100 μM in sample solutions with either TFE: Phosphate buffer (10 mM, pH 7.0) having a volume ratio of 4:6 (v/v), SDS micelles (100 mM) in phosphate buffer (10 mM, pH 7.0), or Single Unilamellar Vesicles (SUVs) of simulated surfactant lipids (DPPC: POPC: POPG; 5:3:2, mole:mole:mole). Surfactant lipid SUVs were prepared at a concentration of 2.6 μM lipids/mL of phosphate buffer solution (10 mM, pH 7.0) by bath sonication for 10 minutes (https://avantilipids.com/tech-support/liposome-preparation/). Sample spectra were baseline corrected by subtracting spectra of protein-free solution from that of the protein-bound solution and expressed as the Mean Residue Ellipticity $[\theta]_{MRE}$ as shown in equation (1):

$$[\theta]_{MRE} = ([\theta]\times 100)/(l\times c\times N) \quad (1)$$

The symbol θ is the measured ellipticity in millidegrees, l is the pathlength in cm, N is the number of residues in the peptide, and c is the concentration of the peptide in mM.

Quantitative estimates of the secondary structural contributions were also made with SELCON 3[29] using the spectral basis set for membrane proteins, option 4 implemented from the DichroWeb website[30,31].

Attenuated-Total-Reflectance Fourier-transform infrared (ATR-FTIR) spectrometry of the B-YL and SMB peptides

ATR-FTIR spectra were recorded at 37°C using a Bruker Vector 22 FTIR spectrometer (Pike Technologies, Fitchburg, WI 53719) with a deuterium triglyceride sulfate (DTGS) detector. The spectra were averaged over 256 scans at a gain of 4 and a resolution of 2 cm^{-1}[14]. For spectra of B-YL and SMB in TFE solutions, self-films were first prepared by air-drying peptide originally in 100% HFIP onto a 50 × 20 × 2 mm, 45° attenuated total reflectance (ATR) crystal for the Bruker spectrometer. The dried peptide self-films were then overlaid with solutions containing 40% TFE/60% deuterated-10 mM sodium phosphate buffer (pH 7.4), at a peptide concentration of 470 μM. Control solvent samples were similarly prepared for FTIR analysis, but without peptide. Spectra of peptides in solvent were obtained by subtraction of the solvent spectrum from that of peptide solvent. For FTIR spectra of B-YL and SMB in either SDS micelles or surfactant lipids, each lipid-peptide solution was transferred onto a germanium ATR crystal. The aqueous solvent was then removed by flowing nitrogen gas over the sample to produce a thick lipid-peptide (lipid:peptide ratios of 10:1, mole:mole)[14]. The multilayer film was then hydrated to ≥35% with deuterated water vapor in nitrogen for 1 h before acquiring the spectra[32]. The spectra for either the B-YL or SMB peptides in the film were obtained by subtracting the spectrum of a peptide-free control sample from that of the peptide-bound sample. The relative amounts of α-helix, β-turn, β-sheet, or random (disordered) structures in lipid-peptide films were estimated using Fourier deconvolution (GRAMS AI 8, version 8.0, Thermo Fisher Scientific, Waltham, MA 02451). The respective areas of component peaks were calculated using curve-fitting software (Igor Pro, version 1.6, Wavemetrics, Lake Oswego, OR 97035)[33]. FTIR frequency limits were: α-helix (1662-1650 cm^{-1}), β-sheet (1637-1613 cm^{-1}), turn/bend (1682-1662 cm^{-1}), and disordered or random (1650-1637 cm^{-1})[34].

Homology models of the structures for B-YL and SMB

Preliminary structural models for SMB and B-YL were determined by analyzing the respective amino acid sequences with a recent homology modeling program[35,36]. The homology three-dimensional (3D) structure for oxidized SMB was obtained by first predicting the reduced SMB structure with a submission of the primary sequence (with four cysteines at residues 8, 11, 34, and 40; Figure 1A) to I-TASSER 5.1 using the automated I-TASSER web service. I-TASSER is a homology algorithm that models discrete regions of the protein using multiple PDB (Protein Data Bank) depositions. The output for a predicted 3D-protein structure was a PDB file, and the accuracy of these models was estimated using such parameters as C-score, TM-score and RMSD[35–37]. The oxidized SMB model was next obtained by using Hyperchem 8.0 (Hypercube, Inc., Gainesville, FL 32601) to convert the four cysteine residues in the reduced SMB model to the known disulfide bonds at Cys-8 to Cys-40 and Cys-11 to Cys-34[14]. The corresponding I-TASSER structure for B-YL was similarly obtained using the SMB sequence (Figure 1A), except with no disulfide linkages due to the replacement of the four Cys residues with Tyr (Figure 1B). Molecular graphics were rendered using Pymol Version 1.7.4.1 (Schrodinger, LLC; San Diego, CA 92121) or MolBrowser-Pro 3.8-3 (Molsoft LLC; San Diego, CA 92121).

Molecular dynamics (MD) simulations of B-YL and SMB in surfactant lipids

The above I-TASSER structures for B-YL and SMB were each modeled as monomers to serve as templates for subsequent all-atom molecular dynamics simulations. Each homology-modeled peptide was oriented in a DPPC:POPC:POPG bilayer with the OPM database and PPM web server[38]. The resulting amphipathic peptide was then uploaded to the Charmm Membrane Builder[39]. The peptide was inserted into a surfactant lipid bilayer having the same proportions of DPPC, POPC, and POPG (64 lipids per monolayer leaflet) as the experimental formulation using the lipid replacement method. The lipid-peptide ensemble was then placed in a 69.19 x 69.12 x 87.00 Å simulation box and hydrated with 2160 TIP3 waters with potassium ions added to render the solution electrically neutral. The simulation box was then downloaded from the Charmm GUI website server using the Gromacs simulation option to set up the system for the equilibration and production runs employing MD simulation structural refinement.

MD simulations were carried out using the Charmm 36 implementation for lipids and proteins in the Gromacs (Version 5.1.1) environment[40] with a Quantum TXR431 workstation (Exxact Corp., Fremont, CA 94539) with an Intel Xeon ES-2650 CPU with two NVIDIA Geforce GTX980 Ti GPU cards. The system was first minimized using a steepest descent strategy followed by a six-step equilibration process at 311°K for a total of 375 ps. This included both NVT (constant number, volume, temperature) and NPT (constant number, pressure, temperature) equilibration phases to allow water molecules to reorient around the lipid headgroups and any exposed parts of the peptide, as well as permitting lipids to optimize their orientation around the peptide. Equilibration protocols employed a PME (Particle Mesh Ewald) strategy for Coulombic long-range interactions and Berendsen temperature coupling. A Berendsen strategy was also used for pressure coupling in a semi-isotropic mode to emulate bilayer motion. After equilibration, the system was subjected to a dynamics production run at the same temperature using the Nose-Hoover protocol and pressure (Parrinello-Rahman) values used in the pre-run steps for a period of 100 ps. The Verlet cut-off scheme was employed for all minimization, equilibration, and production steps. Detailed protocols and parameter files for this type of membrane simulation are available from the Charmm-GUI website v1.7. The output of the production run simulations

was analyzed with the Gromacs suite of analysis tools, while molecular graphics were rendered using Pymol Version 1.7.4.1 or MolBrowser-Pro 3.8-3.

Hydropathy predictions of B-YL and SMB inserting into lipid bilayers through their respective N- and C-terminal α-helices

Membrane Protein Explorer (MPEx; Version 3.2.9) is a program that calculates hydrophobic lipid-protein interactions in membranes. With the hydropathy analysis mode[41], hydropathy plots are produced using the augmented Wimley-White (WW) whole-residue hydrophobicity scale that predicts membrane-bound helices for protein sequences with high accuracy[41–43]. This enhanced scale is based on the experimental partitioning of hydrophobic pentapeptides[44] into *n*-octanol (i.e., a solvent mimic of the hydrocarbon (non-polar) region of the bilayer), and accounts for the whole-residue energy contributions due to the peptide backbone, side chains, and salt-bridge pairs[41,42]. Protein sequences may be submitted to the MPEx program, and the resulting plots are presented as hydropathy (kcal/mol) versus the sequence residue number, averaged over a sliding window of 19 amino-acid residues. Higher positive hydropathy values indicate deeper partitioning in the lipid bilayer for any putative membrane α-helices (e.g., N- and C-terminal helices).

Captive bubble surfactometry

Adsorption and surface tension lowering ability of surfactant preparations were measured with a captive bubble surfactometer at physiological cycling rate, area compression, temperature, and humidity[14]. The captive bubble surfactometer used here was a fully-computerized version of that described and built by Schürch and coworkers[45,46]. We routinely analyze surfactant preparations at an average surfactant lipid concentration of 25 μg/mL and perform all measurements in quadruplicate. We used a B-YL surfactant mixture consisting of 3% of B-YL peptide formulated in surfactant lipids (DPPC:POPC:POPG 5:3:2, mole:mole:mole) with a concentration of 35 mg/mL. Surfactant lipids alone were used as negative control and SMB surfactant (3% of SMB in surfactant lipids) and the clinical surfactant Curosurf® (porcine lung extract containing both SP-B and SP-C and 80 mg/mL of lipids) as positive control.

In vivo experiments

Animal experiments were performed under established protocols reviewed and approved by the Institutional Animal Care and Use Committee of the Los Angeles Biomedical Research Institute at Harbor-UCLA Medical Center (LA BioMed protocol # 020645). All procedures and anesthesia were in accordance with the American Veterinary Medical Association (AMVA) guidelines. Any suffering of the rabbits was ameliorated by providing optimal anesthesia and sedation as outlined below.

The lung lavage rabbit model represents a relatively pure state of surfactant deficiency over at least 6–8 h and allows for serial measures of arterial blood gases and lung compliance in ventilated, surfactant-deficient animals with a clinical picture of respiratory failure as seen in neonatal RDS and ALI/ARDS. Respiratory failure secondary to surfactant deficiency has a high mortality if not treated with a highly surface-active surfactant preparation. Thirty-three young adult, New Zealand white rabbits, weighing 1.0–1.4 kg, were purchased from IFPS Inc. (Norco, CA). The animals were housed as pairs for a minimum of 24 h in the C.W. Steers Biological Resources Center of LA BioMed, using large cages with non-traumatic and moisture absorbent bedding, and provided with rabbit toys and food and water *ad libitum*. Husbandry was provided by veterinary technicians under supervision of a veterinarian. The number of animals has been determined from a population correlation=0.6, α=0.05, tails=2, and power=0.8, which gives a sample size of 16 (2x8). Therefore, we generally use 8 animals to test clinical efficacy of an experimental surfactant preparation (here: 3% B-YL in surfactant lipids, n=9) with groups of 8 animals as positive controls (here: Curosurf® and 3% SMB in surfactant lipids, both n=8) and 8 animals for negative controls (here: surfactant lipids alone [DPPC:POPC:POPG 5:3:2 mole:mole:mole], n=8), as these treatment group sizes allow significant differences to be found between rabbits receiving an optimal surfactant and positive and negative controls. Animals were assigned to a surfactant preparation using a randomized algorithm and experiments were performed in special laboratory area set up for the provision of intensive care.

The rabbits received anesthesia with 50 mg/kg of ketamine and 5 mg/kg of acepromazine intramuscularly prior to placement of a venous line via a marginal ear vein. After intravenous administration of 2 mg/kg of propofol and 2 mg/kg of midazolam for anesthesia and sedation, a small incision in the skin of the anterior neck allowed for placement of an endotracheal tube and a carotid arterial line. After insertion of the endotracheal tube, mechanical ventilation was initiated and muscle paralysis induced with intravenous vecuronium (0.1 mg/kg) to prevent spontaneous breathing. During the ensuing duration of mechanical ventilation, anesthesia consisted of continuous intravenous administration of 30 mg/kg/h of propofol and, as needed, additional intravenous dosages of 2 mg/kg of midazolam for sedation, whereas muscle paralysis was maintained with hourly intravenous administration of 0.1 mg/kg of vecuronium. Maintenance fluid was provided with a continuous infusion of lactated Ringer's solution at a rate of 10 mL/kg/h. Heart rate, arterial blood pressures and rectal temperature were monitored continuously (Labchart® Pro, ADInstruments Inc., Colorado Springs, CO).

The rabbits were ventilated with a volume-controlled rodent ventilator (Harvard Apparatus, South Natick, MA) using a tidal volume 7.5 mL/kg, a positive end-expiratory pressure of 3 cm H_2O, an inspiratory/expiratory ratio of 1:2, 100% oxygen, and a respiratory rate sufficient to maintain the partial pressure of carbon dioxide ($PaCO_2$) at ~40 mmHg. Airway flow and pressures and tidal volume were monitored with a pneumotachograph connected to the endotracheal tube (Hans Rudolph Inc., Kansas City, MO). When the partial pressure of oxygen in arterial blood (PaO_2) was >500 mmHg at a peak inspiratory pressure <15 cm H_2O in 100% oxygen, surfactant deficiency was induced with repeated intratracheal instillation and removal of 30 mL/kg of warmed normal saline. When the PaO_2 was

stable at <100 mmHg (average 4 lavages), B-YL surfactant or a surfactant control (SMB, Curosurf® or surfactant lipids alone) was then instilled intratracheally at a dose of 100 mg/kg body weight and a concentration of 35 mg/mL (80 mg/mL for Curosurf®). Oxygenation was followed by measuring arterial pH and blood gases and lung compliance at 15 min intervals over a 2 h period. Dynamic lung compliance was calculated by dividing tidal volume/kg body weight by changes in airway pressure (peak inspiratory pressure minus positive end-expiratory pressure) (mL/kg/cm H_2O).

Animals were sacrificed 2 h after surfactant administration with an overdose (200 mg/kg) of intravenous pentobarbital. End-points were oxygenation and dynamic lung compliance at 120 min after surfactant administration.

Statistical analysis

All data are expressed as mean ± SEM. Statistical analyses (IBM Statistical Package for the Social Sciences (SPSS) 23.0) used Student's t-test for comparisons of discrete data points, and functional data were analyzed by one-way analysis of variance (ANOVA) with Scheffe's post hoc analysis to adjust for multiple comparisons. Differences were considered statistically significant if the P value was <0.05.

Results

Spectroscopic analysis of B-YL and SMB in lipid mimic and surfactant lipid environments

The secondary structures for B-YL in either lipid mimetics (i.e., 40% TFE/60% deuterated-sodium phosphate buffer, pH 7.4 and deuterated aqueous SDS micelles) or surfactant lipids [i.e., deuterated aqueous DPPC: POPC: POPG 5:3:2 (mole:mole:mole) multilayers] were studied with conventional ^{12}C-FTIR spectroscopy. Representative FTIR spectra of the amide I band for B-YL in these environments were all similar (Figure 2), each showing a principal component centered at ~1654–1655 cm^{-1} with a small low-field shoulder at ~1619–1626 cm^{-1}. Because earlier FTIR investigations of proteins and peptides[34,47] have assigned bands in the range of 1650–1659 cm^{-1} as α-helical, while those at ~1613–1637 cm^{-1} are characteristic of β-sheet, B-YL probably assumes α-helical and β-sheet structures and possibly other conformations in these environments. Self-deconvolutions of the Figure 2 spectra confirmed that B-YL is polymorphic, primarily adopting α-helix but with significant contributions from β-sheet, loop-turn and disordered components (Table 1). Interestingly, the relative proportions of secondary conformations determined from FTIR spectra of B-YL (i.e., α-helix > loop-turn ~ disordered ~ β-sheet) in both lipid-mimetics and surfactant lipids of varying polarity are all comparable, suggesting an overall stability of the B-YL structure that is remarkably conserved. It is also important to note that the proportions of these secondary conformations are all compatible with B-YL principally assuming an α-helix hairpin[10,14,17].

The secondary conformations for B-YL in lipid mimics (i.e., 40% TFE, aqueous SDS) or synthetic surfactant lipids [aqueous (DPPC:POPC:POPG 5:3:2 mole:mole:mole] were also studied with Circular Dichroism (CD) spectroscopy, to validate the above FTIR results. CD spectra for B-YL in these environments (Figure 3) were all similar, each indicating a major α-helical component characterized by a double minimum at 208 and 222 nm[48–50]. Deconvolutions of the Figure 3 spectra showed that B-YL is polymorphic, principally adopting α-helix (~45–52%), but with significant contributions (i.e., ~10–26% each) from loop-turn, disordered/random and β-sheet components (Table 1). Interestingly, the secondary conformation proportions determined from CD analysis for B-YL (i.e., α-helix > random ~loop-turn ~β-sheet) in both surfactant lipids and lipid mimetics are all compatible with B-YL folding as an α-helix hairpin[17]. Moreover, the overall maintenance of these secondary conformations from CD spectra in Table 1 additionally supports our FTIR findings that B-YL assumes a stable 3D-structure in environments of varying polarity.

Comparative FTIR spectroscopic studies were next performed on oxidized Super Mini-B (SMB) in lipid mimics and surfactant lipids to assess whether the B-YL substitutions in Figure 1 perturb the structure of the parent SMB. The secondary structures for SMB in lipid mimetics (i.e., deuterated 40 % TFE, deuterated aqueous SDS) and surfactant lipids (deuterated aqueous DPPC:POPC:POPG 5:3:2 mole:mole:mole) were investigated with conventional ^{12}C-FTIR spectroscopy. Figure 4 shows that representative FTIR spectra of the amide I band for SMB in these environments were similar, each indicating a dominant α-helical component centered at ~1654–1655 cm^{-1} with a small low-field shoulder due to β-sheet at ~1618–1620 cm^{-1}[134,47]. Self-deconvolution of the FTIR spectra in Figure 4 demonstrated that SMB in either TFE, SDS or surfactant lipids folds with secondary structures that are characteristic of the α-helix hairpin (Table 1). Our finding that the respective secondary structure profiles for B-YL and SMB are similar in Table 1 suggests that the amino-acid substitutions in B-YL (e.g., four Cys residues replaced by Tyr) do not disrupt the α-helix hairpin conformation. Instead, these results raise the possibility that the replacement Tyr residues may stabilize the B-YL fold via a core of clustered tyrosines linking the N- and C-α-helices through noncovalent interactions involving aromatic rings (*see below*).

Molecular dynamics (MD) simulations of B-YL in a lipid environment

MD simulations were subsequently conducted to obtain residue-specific information on B-YL in a surfactant lipid bilayer-water box. Although the above ^{12}C-FTIR results on SP-B mimics (i.e., B-YL and SMB) are useful for experimentally assessing secondary structures averaged over the entire peptide, they cannot indicate the conformations of individual amino acids. With starting models based on homologous structures, however, MD runs in the Gromacs environment should provide our most accurate estimates of not only the 3D-conformations of SP-B mimics, but also the molecular topography of these peptides in the hydrated lipid bilayer. In the present work, MD simulations on B-YL were begun by first predicting the homologous 3D-structure by submitting the B-YL sequence (Figure 1B) to the I-TASSER web service. Three distinct models for B-YL were obtained from I-TASSER Version 5.1, and Model 1 with

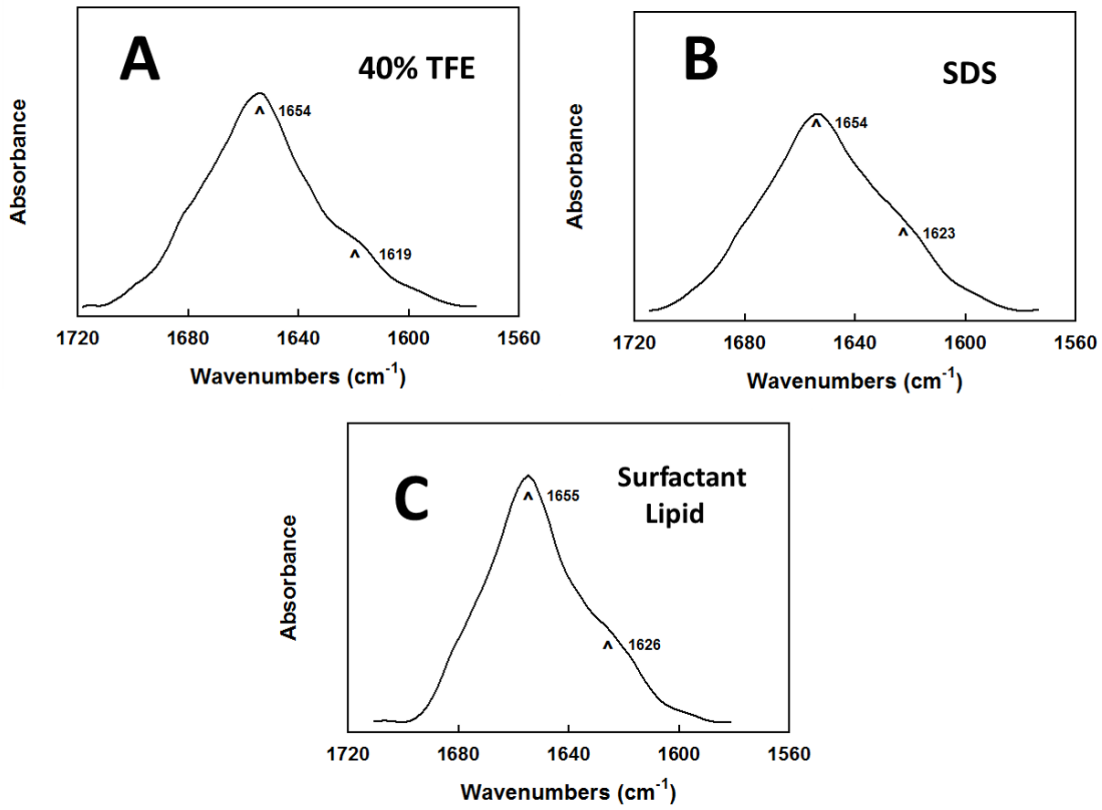

Figure 2. FTIR spectra of the B-YL mimic in several lipid-mimetics and surfactant lipids. Attenuated total reflectance Fourier transform infrared (ATR-FTIR) spectral plots show the absorbance (in arbitrary units) as a function of wavenumbers (cm^{-1}) (See **Methods** and **Results**). (**A**) Deuterated aqueous 40% TFE. (**B**) Deuterated aqueous SDS. (**C**) Deuterated aqueous surfactant lipid. In (**A**), (**B**) and (**C**), the IR spectra each show dominant α-helical components centered at 1654–1655 cm^{-1} (arrows), with minor bands at ~1619–1626 cm^{-1} (arrows) due to β-sheet, ~1682–1662 cm^{-1} due to loop-turn/bend, and ~1650–1637 cm^{-1} due to disordered or random conformations. Peptide concentrations were 470 μM for the TFE solvent spectra, and 10:1 lipid:peptide (mole:mole) for the SDS detergent and surfactant lipid spectra. The areas under each absorbance curve are normalized.

the highest C-score was selected (*not shown*). The accuracy of Model 1 was estimated from the following parameters: C-score of -0.73, TM-score of 0.62 ± 0.14 and RMSD of 3.6 ± 2.5 Å. C-score is a confidence score for evaluating the quality of I-TASSER models (between -5 to 2), with elevated values indicating a model with high confidence[35,36]. TM-score is a scale quantifying the similarity between two structures, with scores >0.50 signifying a model of correct topology and scores <0.17 implying random similarity[35–37,51]. Moreover, root mean square deviation (RMSD) is an average distance of all residue pairs in the two structures. The high C- and TM-scores, combined with the low RMSD, indicate that Model 1 will provide useful initial estimates of the secondary and tertiary structures for B-YL.

The resulting I-TASSER model for B-YL (*not shown*) predicts a C-terminal α-helix (residues P30-V37) connected to an N-terminal helix (residues Y8-L21) via a coil (residues I22-L29), which assumes a helix hairpin conformation[52,53]. The putative helix hairpin of B-YL executes a reverse turn after 8-residues with the I22-G25 component being the most prominent. Comparable to prior helix hairpins[54], homology analysis of the B-YL sequence indicated high β-turn propensities for I22 to G25, allowing close interactions between the hydrophobic interfaces of the nearly antiparallel N- and C-helices. The helix hairpin fold of B-YL may be stabilized by a general increase in hydrophobicity due to Tyr and Leu substitutions (Figure 1A, B). Enhanced helix hairpin folding may also be due to the formation of clustered Tyr residues (i.e., Y7, Y8, Y11, Y34, and Y40) in the protein interior linking together the N- and C-helices through noncovalent interactions involving aromatic rings (*not shown*). The driving force behind this Tyr networking is at least partly due to "π-stacking" interactions of neighboring aromatic groups[55,56], which were frequently observed in a survey of proteins deposited in the PDB[57]. Interestingly, Y7, Y8, and Y40 are oriented in a "pinwheel" arrangement with a 3-fold axis inside the protein core, similarly to how π-stacking interactions optimally organize benzene trimers in an early molecular mechanics study[57]. A second π-stacked configuration for the remaining Tyr residues was identified immediately adjacent to the pinwheel trimer, in which Y34 and Y11 nearly adopt a 1p dimer configuration with their tyrosine rings off-centered and parallel displaced[55,57]. The I-TASSER model further forecasts a flexible coil for the

Table 1. Spectroscopic proportions of secondary structure[a] for B-YL and SMB in lipid-mimetics and surfactant lipid.

System	% Conformation[a]			
	α-Helix	Loop-Turn	β-Sheet	Disordered
FTIR Analysis of B-YL[b]				
40% TFE	44.9	20.1	14.0	21.0
SDS	43.5	21.5	15.4	19.6
Surfactant Lipid	44.3	18.9	15.1	21.7
CD Analysis of B-YL[c]				
40% TFE	46.9	11.8	15.1	26.2
SDS	52.0	13.9	9.9	24.2
Surfactant Lipid	44.6	16.3	13.3	25.8
FTIR Analysis of SMB[d]				
40% TFE	47.1	19.4	20.2	13.3
SDS	44.9	22.2	12.2	20.7
Surfactant Lipid	42.3	27.5	11.7	18.5

[a]Tabulated results are means from four closely-reproduced separate determinations for each condition and spectral type.

[b]See Figure 2. ATR-FTIR spectra were estimated for proportions of the secondary structure for B-YL in 40% trifluoroethanol (TFE), sodium dodecyl sulfate SDS micelles and surfactant lipid-MLV films using self-deconvolution of the peptide amide I band (see **Methods** and **Results**).

[c]See Figure 3. Circular dichroism (CD) spectra were analyzed for proportions of the secondary structure for the B-YL mimic in 40% TFE, SDS micelles or surfactant lipid using spectral deconvolution (see **Methods** and **Results**).

[d]See Figure 4. ATR-FTIR spectra were estimated for proportions of the secondary structure for the oxidized Super Mini-B (SMB) in SDS micelles and surfactant lipid-MLV films using self-deconvolution of the peptide amide I band (see **Methods** and **Results**).

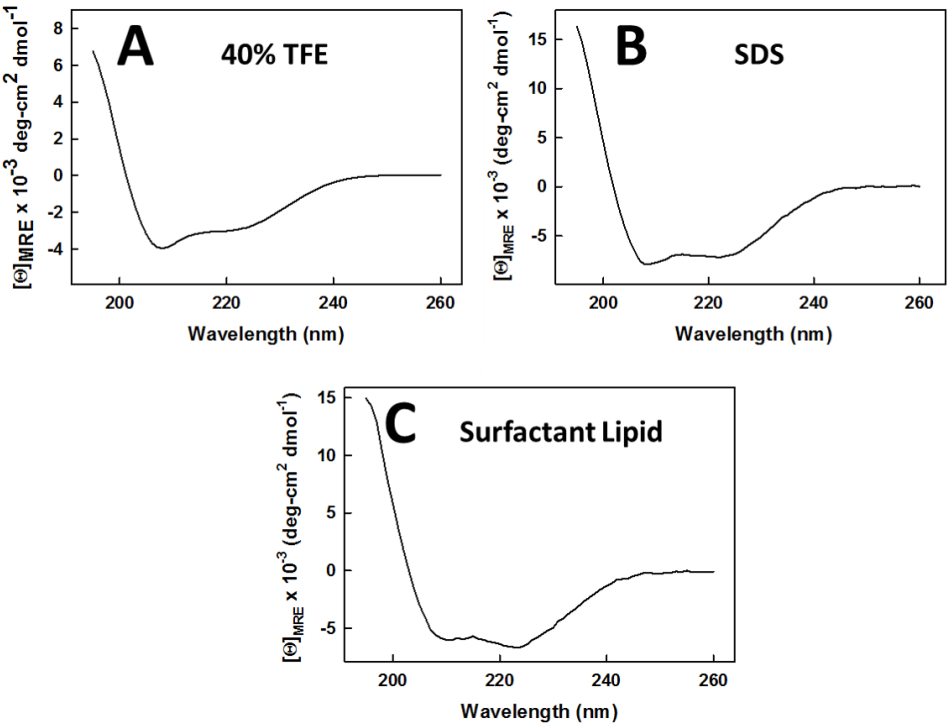

Figure 3. CD spectra of the B-YL mimic for SP-B in several lipid-mimetics and surfactant lipid. Circular Dichroism (CD) spectral plots show the mean residue ellipticities ($[\theta]_{MRE}$ x 10^{-3} deg-cm^2 dmol^{-1}) as a function of wavelength (nm). (**A**) 40% TFE. (**B**) SDS. (**C**) Surfactant Lipid. The double minimum at 208 and 222 nm in each plot indicates that α-helix is the dominant secondary structure for B-YL in these environments. Peptide concentrations were 100 μM. The optical pathlength was 0.01 cm and the temperature was 37°C. Spectra represent the average of 8 scans.

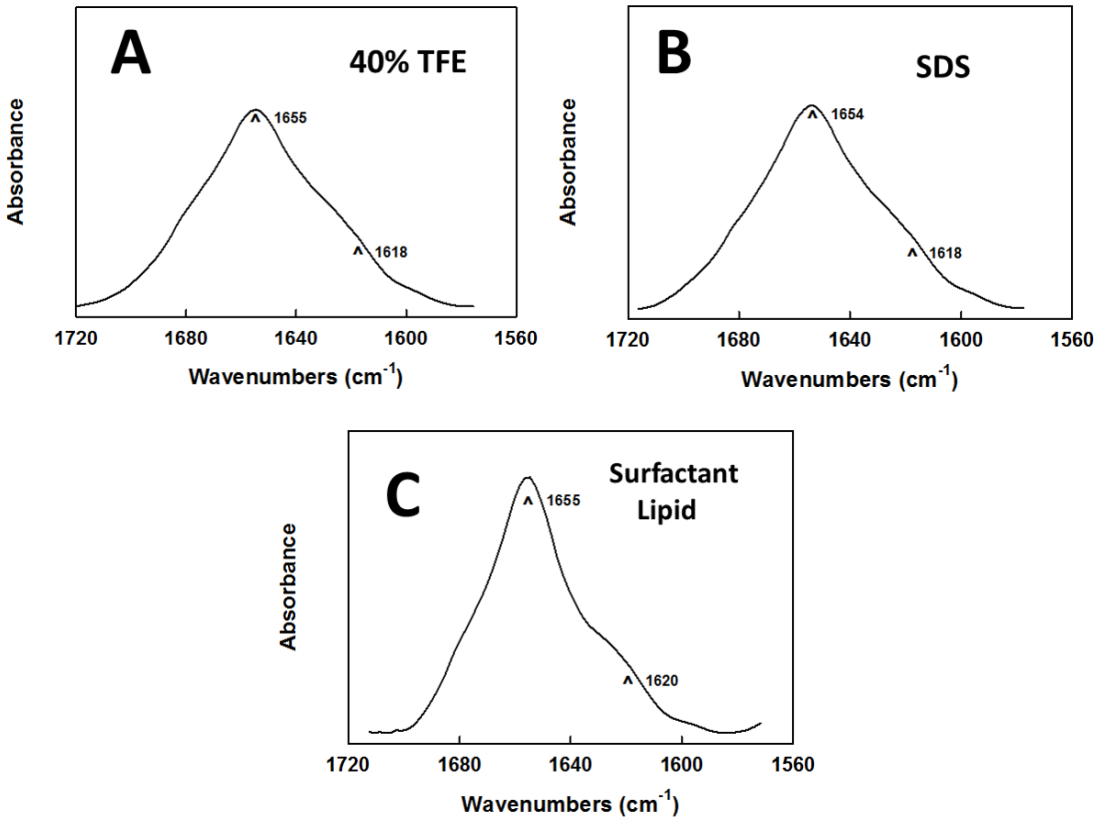

Figure 4. FTIR spectra of the oxidized Super Mini-B (SMB) in several lipid-mimetics and surfactant lipids. Attenuated total reflectance Fourier transform infrared (ATR-FTIR) spectral plots show the absorbance (in arbitrary units) as a function of wavenumbers (cm^{-1}) (See **Methods** and **Results**). (**A**) Deuterated aqueous 40% TFE. (**B**) Deuterated aqueous SDS. (**C**) Deuterated aqueous surfactant lipid. In (**A**), (**B**) and (**C**), the IR spectra each show dominant α-helical components centered at 1654–1655 cm^{-1} (arrows), with minor bands at ~1618–1620 cm^{-1} (arrows) due to β-sheet, ~1682–1662 cm^{-1} due to loop-turn/bend, and ~1650–1637 cm^{-1} due to disordered or random conformations. Peptide concentrations were 470 μM for the TFE solvent spectra, and 10:1 lipid:peptide (mole:mole) for the SDS detergent and surfactant lipid spectra. The areas under each absorbance curve are normalized.

N-terminal insertion sequence (F1-P6), which permits this hydrophobic segment to interact with the π-stacked tyrosine residues within the B-YL interior. Lastly, the space-filling I-TASSER model indicates that the folding of B-YL into a helix hairpin produces a compact globular protein, exhibiting a core of hydrophobic residues and a surface of aqueous-exposed and polar residues (*not shown*).

MD simulations of B-YL were next calculated by porting the above I-TASSER Model 1 into aqueous DPPC:POPC:POPG bilayers with potassium counterions to maintain electrical neutrality. This lipid mixture was chosen for *in silico* studies because it optimizes the surfactant activity of our SP-B mimics in both *in vitro* and *in vivo* assays. Simulations were then carried out for 0–500 nsec using the Charmm 36 implementation for lipids in the Gromacs (Version 5.1.1) environment[40]. The representative "500 nsec" structure for B-YL in lipids (Figure 5A) largely agrees with the I-TASSER model on which it is based. Similar to the original I-TASSER model, Figure 5A indicates that the "500 nsec" model in surfactant lipids is folded as a helix-hairpin-helix, in which an N-terminal α-helix (residues R12-L21) connects to a C-terminal α-helix (P30-L36) via a turn-loop (I22-L29). The high β-turn propensity of B-YL in Figure 5A (i.e., P23 – G26; green wire sidechains) allows close interaction between the hydrophobic interfaces of the nearly antiparallel N- and C-helices. The 500 ns B-YL model also predicts flexible coils for the N-terminal insertion (F1 – Y11) and the C-terminal (V37 – S41) sequences. Lastly, space-filling I-TASSER and 500 ns MD simulation models for B-YL each produced a compact globular protein, exhibiting a core of hydrophobic residues and a surface of aqueous-exposed and polar residues (*not shown*).

Although major changes were not observed between the I-TASSER and 500-nsec models for B-YL, there were nevertheless significant minor differences which we attribute to the

500 nsec-equilibration of the I-TASSER structure in the aqueous lipid-bilayer box. For example, note that the N α-helix of the "500 nsec" model is shorter by four residues, with Y8, W9, L10, and Y11 not participating in the N α-helix. Concurrently with the fraying of the N-helix by one turn, there is a reorganization of the five tyrosine residues in the "500 nsec" model. Namely, the pinwheel trimer and 1p dimer in the I-TASSER B-YL model convert to a distorted pinwheel trimer (i.e., Y8, Y11 and Y34) in the hydrophobic interior of the 500 nsec B-YL, with Y7 and Y40 migrating to the polar surface (Figure 5A). The approximate 3-fold axis relating the three tyrosines is seen more clearly by reorienting the 500 nsec model so that the symmetry axis is perpendicular to the plane of the paper (see "X"), with the Tyr representations in purple stick (Figure 6A) and space-filling (Figure 6B), respectively. This three-fold axis is designated an "approximate" symmetry axis because it is strictly valid for all three tyrosine ring structures, but not for the hydroxyl of Y8, which faces an opposite direction than those of the hydroxyls for either Y11 or Y34 (Figure 6A, B). Figure 6 confirms that the 500 nsec model B-YL folds as a helix hairpin, with the approximate pinwheel trimer (Y8, Y11, and Y34) bridging together the N- and C-α helices through non-covalent interactions. The space-filling 500 nsec model for B-YL further demonstrates a globular protein, in which the pinwheel Tyr trimer embeds with other hydrophobic residues in the interior, while hydrophilic groups face the exterior (*not shown*). Notably, the pinwheel Tyr trimer in Figure 6 may act as a hydrophobic core around which other hydrophobic residues assemble, but from which all water is absent. Because water disrupts secondary structure by attacking amide-amide hydrogen bonds, the stability of the B-YL conformation for 500 nsec in Figure 5A and Figure 6 may be due not only to non-covalent interactions between hydrophobic residues (e.g., π-stacking of Tyr residues) but also to water exclusion from the hydrophobic interior (i.e., solvophobic forces)[55,56].

The topological organization of B-YL in the membrane bilayer may also be characterized using the above all-atom (500 nsec) MD simulation of B-YL in hydrated lipid surfactant (DPPC: POPC:POPG 5:3:2 mole:mole:mole) at 37°C. Figure 7A shows a cross-sectional view of the ribbon model for the 500 nsec B-YL in the lipid bilayer. Here, the buried Y8, Y11 and Y34 tyrosines (i.e., purple stick sidechains) bridge the N- and C-α helices through noncovalent aromatic interactions, while the surface-exposed Y7 and Y40 interact with water molecules or polar lipid headgroups (see also Figure 5A). The axes for the N- and C-α helices are each nearly parallel to the bilayer plane. However, the N-α helix lies deeper in the bilayer subjacent to the lipid headgroup, while the C-α helix binds to the more polar lipid-water interface (Figure 7A). This differential partitioning may be just due to differences in the hydrophobicities of the two helices because MPEx analysis[41] indicated a higher hydropathy (i.e., more hydrophobic) for the N-α-helix than for the C-α helix (i.e., 4.92 *vs.* -0.02 kcal/mol, respectively). The 500 nsec – MD simulation model for B-YL in aqueous surfactant lipids also demonstrated the absence of any water or lipid within its hydrophobic core (*not shown*). The systematic exclusion of water from the protein interior mediated by the three "π-stacked" tyrosine residues may account for why B-YL folds as a helix-hairpin for simulation times (t) =500 nsec.

Importantly, partial validation of the 500 nsec MD structure for B-YL in aqueous surfactant lipids (Figure 5A) is provided by our above spectroscopic findings. The secondary structures obtained from either FTIR or CD spectra of B-YL in surfactant lipids (Figures 2C and Figure 3C; Table 1) are generally in good agreement with those predicted in the 500 nsec model (Figure 5A). For example, Figure 8A indicates that the respective proportions of secondary structures for B-YL obtained from FTIR self-deconvolutions are compatible with those determined using MD simulations, with the experimental and theoretical techniques each showing high α-helix and smaller contributions due to loop-turn, disordered and β-sheet. These results indicate experimental confirmation of critical features for our MD model of B-YL folding as an α-helix-hairpin (Figure 5A).

Molecular dynamics (MD) simulations of SMB in a lipid environment

MD simulations were likewise performed on oxidized Super Mini-B (SMB) in the surfactant lipid bilayer, to more directly assess whether the amino-acid replacements in B-YL (i.e., four Cys residues substituted with Tyr and two Met residues with Leu) significantly perturbed the α-helix hairpin conformation or its insertion in the hydrated lipid bilayer. As with B-YL, MD simulations on SMB were started by first predicting the homologous 3D-structure by submitting the reduced SMB sequence (Figure 1A, but without the disulfide bonds) to the I-TASSER web service (*see* **Methods**). Four separate models for reduced SMB were obtained from I-TASSER Version 5.1, and Model 1 with the highest C-score was selected for further analysis. Model 1 was estimated to be the most accurate of the four models using the following parameters: C-score of 0.01, TM-score of 0.71 ± 0.11 and RMSD of 2.3 ± 1.8 Å (*see above* and **Methods**)[35–37,51]. The I-TASSER Model 1 for the reduced SMB predicts a C-terminal α-helix (residues P30-L36) connected to an N-terminal helix (residues C8-M21) via a loop-turn (residues I22-R27), which adopts a helix hairpin conformation. Because the distances between two sulfur atoms in the C8-C40 and C11-C34 pairings are only 3.5 and 5.0 Å, respectively, Hyperchem 8.0 readily forms oxidized SMB by converting the four cysteine residues in reduced SMB to the known disulfide bonds.

The above oxidized SMB was then ported into the hydrated surfactant lipid bilayer, and MD simulations were run for 0–500 nsec, permitting detailed structural comparisons between the parent SMB and its daughter peptide B-YL. Figure 5B shows a representative "490 nsec" structure for SMB folding as a α-helix hairpin, with an N-terminal α-helix (i.e., red N-α, residues Y7 – M21) connecting to a C-terminal α-helix (i.e., residues P30 – L36) via a turn (i.e., residues I22 – L29). Experimental support for this helix-hairpin model comes from ^{12}C-FTIR

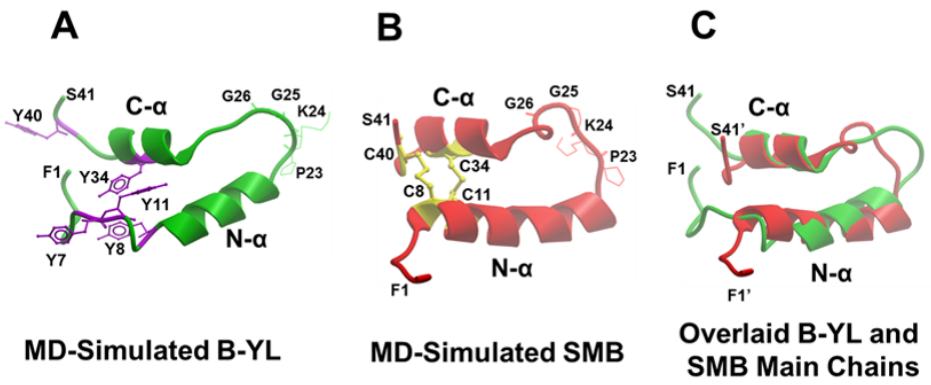

Figure 5. The evolved 3D models for B-YL and SMB in lipid bilayers after MD simulations. Molecular Dynamics (MD) simulations were carried out on the Super Mini-B mimic (B-YL) and oxidized Super Mini-B (SMB) (see **Methods** and **Results**). Main-chain folding of peptides is displayed in ribbon format, with lipids and water omitted for clarity. (**A**) The green ribbon MD model for B-YL is shown, in which Tyr replaces Cys at residues 8, 11, 34, and 40 of the parent SMB with purple stick sidechains (see Figure 1). This 500 nsec simulation predicts a helix-hairpin, in which an N-terminal α-helix (i.e., green N-α, residues R12 – L21) connects to a C-terminal α-helix (i.e., green C-α, residues P30 – L36) via a turn (green residues I22 – L29). The B-YL model also predicts flexible coils for the N-terminal insertion (F1 – Y11) and the C-terminal (V37 – S41) sequences. The B-YL fold is stabilized by a hydrophobic core of clustered Tyr (Y8, Y11, and Y34) linking together the N- and C-helices through noncovalent interactions involving aromatic rings. (**B**) The ribbon model for SMB at 490 nsec forecasts a helix-hairpin conformation, in which an N-terminal α-helix (i.e., red N-α, residues Y7 – M21) connects to a C-terminal α-helix (i.e., red C-α, residues P30 – L36) via a turn (red residues I22 – L29). The SMB model also predicts flexible coils for the N-terminal insertion (F1 – P6) and the C-terminal (V37 – S41) sequences. SMB is oxidized with covalent disulfides (i.e., C8–C40, and C11–C34; yellow stick and ribbon figures) lying deep inside the hydrophobic core. (**C**) The ability of the B-YL peptide to mimic the helix-hairpin folding of its parent SMB was tested with a superimposition of the ribbon backbone of SMB (red) with that of B-YL (green).

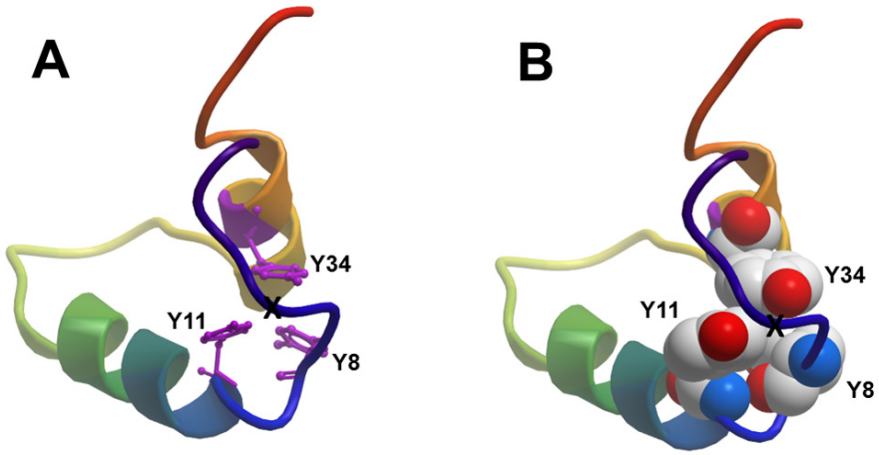

Figure 6. The N- and C-helices of 500 nsec B-YL crosslinked by a symmetry-related tyrosine trimer. Graphical modeling and MD simulations were carried out as described in Figure 5A and **Methods**. Main-chain folding of 500 nsec B-YL is shown in the ribbon-rainbow format, with the N-terminal insertion sequence in blue, the N-terminal helix in blue-green, the turn hairpin in green yellow and the C-terminal helix in yellow-orange. Three of the tyrosine residues (i.e., Y8, Y11, and Y34) are organized as a distorted pinwheel trimer in the hydrophobic interior of the 500 nsec B-YL that links together the N- and C-helices through non-covalent interactions. An approximate 3-fold axis relating the three tyrosines in Figure 5A is seen more clearly by rotating the 500 nsec model so that the symmetry axis is perpendicular to the plane of the paper (see "X"). This three-fold axis is designated an "approximate" symmetry axis because it is strictly valid for all three tyrosine ring structures, but not for the hydroxyl of Y8, which faces an opposite direction than those of the hydroxyls for either Y11 or Y34. (**A**) Graphical representation of the rotated 500 nsec B-YL model is in ribbon-rainbow format, with tyrosine sidechains as purple sticks. (**B**) Graphical representation of the rotated 500 nsec B-YL model is in ribbon-rainbow format, with tyrosine sidechains as space-filling (CPK).

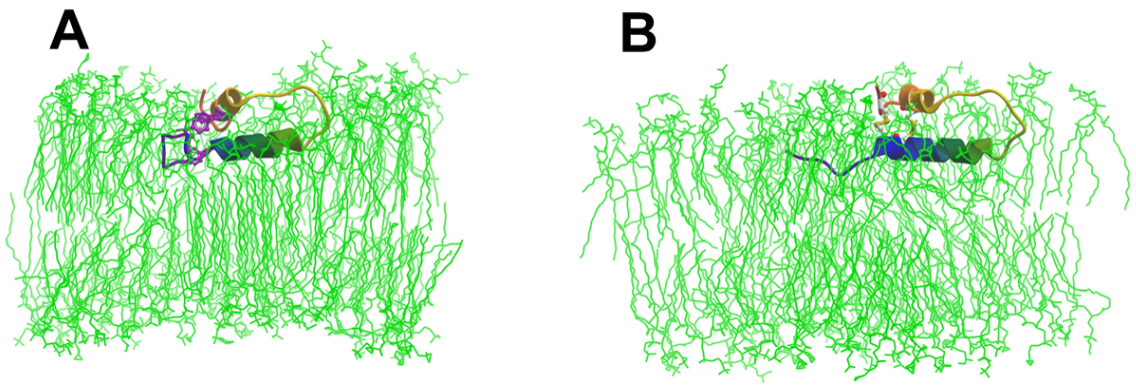

Figure 7. Cross-sectional views of the B-YL and SMB peptides in lipid surfactant bilayers after MD simulations. Graphical modeling and MD simulations were carried out as described in Figure 5 and **Methods**. Main-chain folding for peptides is shown in the ribbon-rainbow format, with the N-terminal insertion sequence in blue, the N-terminal helix in blue-green, the turn hairpin region in green-yellow and the C-terminal helix in yellow-orange. Lipids are shown as green stick figures, while water is left out for clarity. (**A**) The ribbon model for the 500 nsec B-YL conformer folds as a helix-hairpin, with the Y8, Y11 and Y34 tyrosine residues (i.e., purple stick figures) bridging the N- and C-α helices through noncovalent aromatic interactions. The axes for the N- and C-α helices are each nearly parallel to the bilayer plane. However, the N-α helix lies deeper in the bilayer subjacent to the lipid headgroup, while the C-α helix binds to the more polar lipid-water interface. (**B**) The ribbon model for the 499 nsec SMB conformer also adopts a helix-hairpin structure, with the disulfide bonds (i.e., two yellow stick figures) covalently linking the N- and C-α helices. The respective topographical organizations for SMB and B-YL are both similar. Namely, the axes for the N- and C-α helices of SMB are each nearly parallel to the bilayer plane. Moreover, the N-α helix of SMB lies deeper in the bilayer beneath the lipid headgroup, while the corresponding C-α helix binds to the more polar lipid-water interface.

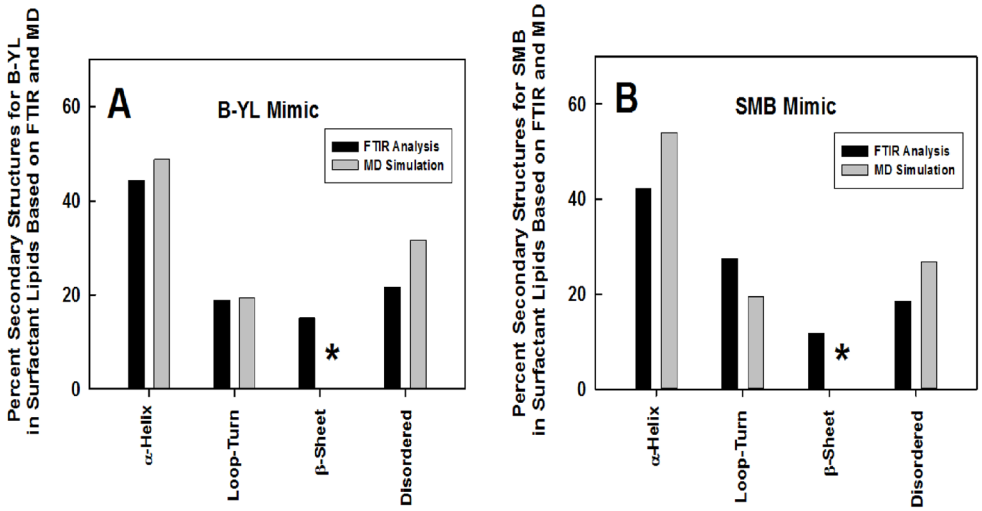

Figure 8. Spectroscopic and MD simulation comparisons of secondary structures for B-YL and SMB in lipids. The SMB mimic is oxidized Super Mini-B with covalent disulfide bonds at C8–C40 and C11–C34, while the B-YL mimic lacks disulfide linkages with Tyr substituted for Cys at residues 8, 11, 34 and 40 and also Leu replacing Met at residues 21 and 28 (*see* Figure 1). (**A**) Plot of % conformations assessed from FTIR spectra (***black bars***) of the B-YL mimic in DPPC:POPC: POPG (5:3:2 mole:mole:mole) bilayers (Table 1) ***vs.*** the corresponding structures calculated from DSSP analysis (i.e., H-bond estimation algorithm) of an MD simulation of B-YL (*gray bars*) in an aqueous DPPC:POPC:POPG lipid box for 500 nsec. The respective proportions of secondary structures for B-YL obtained from FTIR deconvolution are in good agreement with those determined using MD simulations, with each technique showing α-helix > Loop-Turn ~ Disordered = β-sheet. The absence of any β-sheet in our MD model is shown by the asterisk (*). (**B**) Plot of % conformations assessed from ATR-FTIR spectra (*black bars*) of the SMB mimic in DPPC:POPC: POPG (5:3:2 mole:mole:mole) bilayers (see Table 1) *vs.* the corresponding structures calculated from DSSP analysis of an MD simulation of SMB (*gray bars*) in an aqueous DPPC:POPC:POPG lipid box for 490 nsec. The respective proportions of secondary structures for SMB obtained from FTIR spectral deconvolution are comparable to those determined with MD simulations, with each technique showing α-helix > Loop-Turn ~ Disordered ≥ β-sheet. The absence of any β-sheet in our MD model is shown by the asterisk (*).

spectroscopy, in which self-deconvolutions obtained from spectra of SMB in lipid surfactant indicated high α-helix and smaller components due to loop-turn, disordered and β-sheet (Figure 4C and Figure 8B; Table 1)[17]. The helix-hairpin for the 490 nsec model (Figure 5B) produces a reverse turn after 8-residues with the P23-G26 component (red wire sidechains) being the most prominent. Similar to earlier helix-hairpins, the 490 nsec model indicated high β-turn propensities for I22 to G25, allowing close interactions between the hydrophobic interfaces of the nearly antiparallel N- and C-helices. The oxidized SMB additionally predicts flexible coils for the N-terminal insertion (F1 – P6) and the C-terminal (V37 – S41) sequences, as well as covalent disulfides (i.e., C8–C40 and C11–C34) deep within the hydrophobic core that bridge together the N – and C – α-helices. The space-filling 490 nsec model for SMB (*not shown*) additionally indicates a globular protein, in which the hydrophobic disulfide bonds embed with other hydrophobic residues in the interior to quantitatively exclude water, while hydrophilic groups face the exterior. Given that water perturbs secondary structures by attacking amide H-bonds, the stability of the SMB conformation for 490 nsec in Figure 5B may be due not only to covalent disulfide bonds and non-covalent interactions between hydrophobic residues but also to water exclusion from the protein interior (e.g., solvophobic forces)[17,55,56]. Lastly, the insertion of SMB into the lipid bilayer was assessed using an all-atom MD simulation (i.e., a 499 nsec conformer) of SMB in the hydrated lipid surfactant at 37°C. Figure 7B indicates a cross-sectional view of the ribbon model for the 499 nsec SMB in the lipid bilayer, in which the axes for the N- and C-α-helices are each nearly parallel to the bilayer plane. Nevertheless, the N- α helix lies more buried in the bilayer underlying the lipid headgroup, while the C- α helix binds to the more polar lipid-water interface (Figure 7B). MPEx analysis of SMB indicated higher hydropathy (i.e., more hydrophobic) for the N- α-helix than for the C- α-helix (i.e., 3.55 *vs.* 1.87 kcal/mol, respectively)[41], and this may be responsible for the deeper penetration of the N- α-helix into the bilayer.

Comparison of the equilibrated MD-simulation models of B-YL and SMB in lipid surfactant bilayers

Head-to-head comparisons were next conducted on MD simulated models of B-YL and its parent SMB in hydrated lipid surfactant bilayers at ~500 nsec, to determine whether the amino-acid replacements in B-YL significantly perturbed the α-helix hairpin conformation or its insertion in the lipid bilayer. The 500 nsec model of B-YL in Figure 5A is very similar to the corresponding 490 nsec model of the parent SMB in Figure 5B, except for the fraying of the N-terminus of the N-α helix (residues 8-11; one turn), and also the substitution of a distorted tyrosine pinwheel (i.e., purple Y8, Y11, and Y34) that draws together the C-α and N-α helices in Figure 5A instead of the two disulfide linkages (i.e., yellow C8–C40 and C11–C34) in Figure 5B. The fraying of the N-α helix occurs concurrently with the formation of the distorted tyrosine pinwheel in B-YL, suggesting that an unwinding of one helical turn is energetically required to accommodate the tyrosine reorganization of B-YL in Figure 5A. Interestingly, the location of the distorted tyrosine pinwheel in B-YL (Figure 5A and Figure 6) overlaps that of the C11–C34 disulfide bond in SMB (Figure 5B), suggesting that the tyrosine trimer is well positioned to promote the α-helix hairpin conformation in B-YL (see above and Figure 6). The ability of the B-YL peptide to mimic the helix-hairpin folding of its parent SMB was further tested with the automated multiple structural superposition tools in the MolBrowserPro environment. Figure 5C shows a weighted iterative superposition that was performed with the visible atoms of the aligned residues, using SMB as the static object. The output of the superimposition in Figure 5C is shown with the ribbon backbone of SMB (red) overlaid with that of B-YL (green). There is good overlap between the two structures, with the best seen in the stable N- and C-helical cores and less agreement between the more flexible turn and N- and C-terminal regions. These results indicate that the tyrosine substitutions create a B-YL daughter peptide that successfully mimics essential helix-hairpin features of the parent SMB. Because high *in vitro* and *in vivo* surfactant activities are associated with SMB adopting an α-helix hairpin conformation[10,14,17], it will be worthwhile to investigate similar functional correlates with B-YL.

Another direct comparison was performed on MD simulated models of B-YL and SMB in hydrated lipid surfactant bilayers, to assess if the amino-acid substitutions in B-YL disturbed its topological organization in the lipid bilayer (Figure 7A, B). As noted above, Figure 7B shows a cross-sectional view of 499 nsec SMB in the lipid bilayer, in which the N- and C-α-helices are each nearly parallel to the bilayer plane, but the N-α helix lies deeper in the bilayer than the disulfide-linked C-α helix. The corresponding view of 500 nsec B-YL (Figure 7A) demonstrates insertion of its α-helix hairpin into the lipid bilayer which is remarkably analogous to that of 499 nsec SMB (Figure 7B). Accordingly, B-YL and SMB may be each classified as a tightly bound peripheral membrane protein, which interacts with superficial portions of the phospholipid bilayer and lacks transmembrane segments that span the width of the bilayer. The finding of similar topological organizations for B-YL and SMB in the lipid bilayer provides further support for the hypothesis that B-YL may likewise mimic the surfactant activities of SMB (*see below*).

Captive bubble surfactometry

Captive bubble surfactometry of B-YL and SMB surfactants (3% peptide in DPPC:POPC:POPG 5:3:2 mole:mole:mole), Curosurf®, and surfactant lipids alone demonstrated excellent surface activity of B-YL (Figure 9). Surface activity of BYL and SMB surfactant and Curosurf® were consistently and equally low during quasi-static cycling with values ≤1 mN/m, indicating that the modifications in the B-YL peptide did not lead to a loss in *in vitro* surface activity compared to its parent peptide SMB. In contrast,

minimum surface tension values of surfactant lipids alone far exceeded those of B-YL, SMB and Curosurf® surfactant and amounted to ~18 mN/m ($p<0.001$).

In vivo experiments

Animal experiments directly examined the *in vivo* pulmonary activity of B-YL surfactant when instilled intratracheally in ventilated young adult rabbits with surfactant deficiency and impaired lung function induced by repeated saline lung lavages (Figure 10). Surfactant was administered by intratracheal instillation after the PaO_2 was reduced to stable levels <100 mmHg, which is far below the threshold clinical criteria for ARDS of a PaO_2 <200 mmHg and for ALI of <300 mmHg when breathing 100% oxygen. For this timeframe of study, this model reflects a relatively pure state of surfactant deficiency in animals with mature lungs. Rabbits receiving B-YL, SMB and Curosurf® surfactant had significantly improved arterial oxygenation over the 2 h period of study post-instillation compared to control rabbits instilled with surfactant lipids alone (Figure 10, $p<0.001$). Dynamic lung compliance also significantly improved over the same period of post-instillation study in rabbits treated with B-YL and SMB surfactants and Curosurf® compared to lipid-only controls (Figure 10). The differences between B-YL and SMB surfactants and Curosurf® were not statistically significant, indicating that the modifications in the SP-B peptide mimic B-YL did not lead to a loss in *in vivo* surface activity.

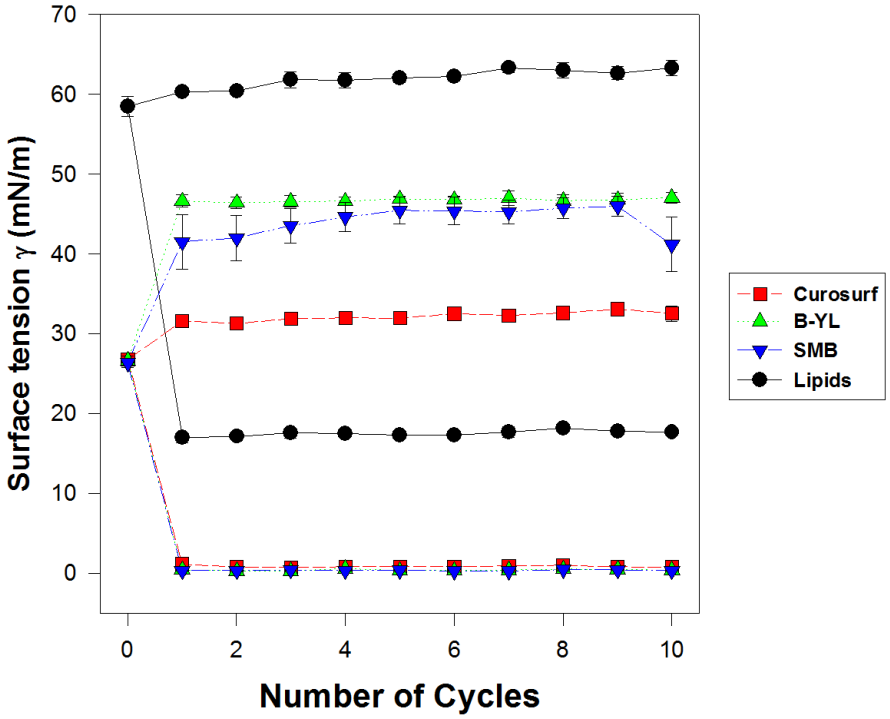

Figure 9. Surface tension reduction activity measured with captive bubble surfactometry. Surface activity of 3% B-YL and oxidized Super Mini-B (SMB) in surfactant lipids were compared with a clinical surfactant (Curosurf®) as positive control and surfactant lipids alone (DPPC:POPC:POPG 5:3:2 mole:mole:mole) as negative control. The lower part of each curve indicates minimum surface tension and the upper part indicates maximum surface tension during 10 compression-expansion cycles. Minimum surface tension values of B-YL and SMB surfactant were similar to those of Curosurf®. Values are mean ± SEM of N=4-5.

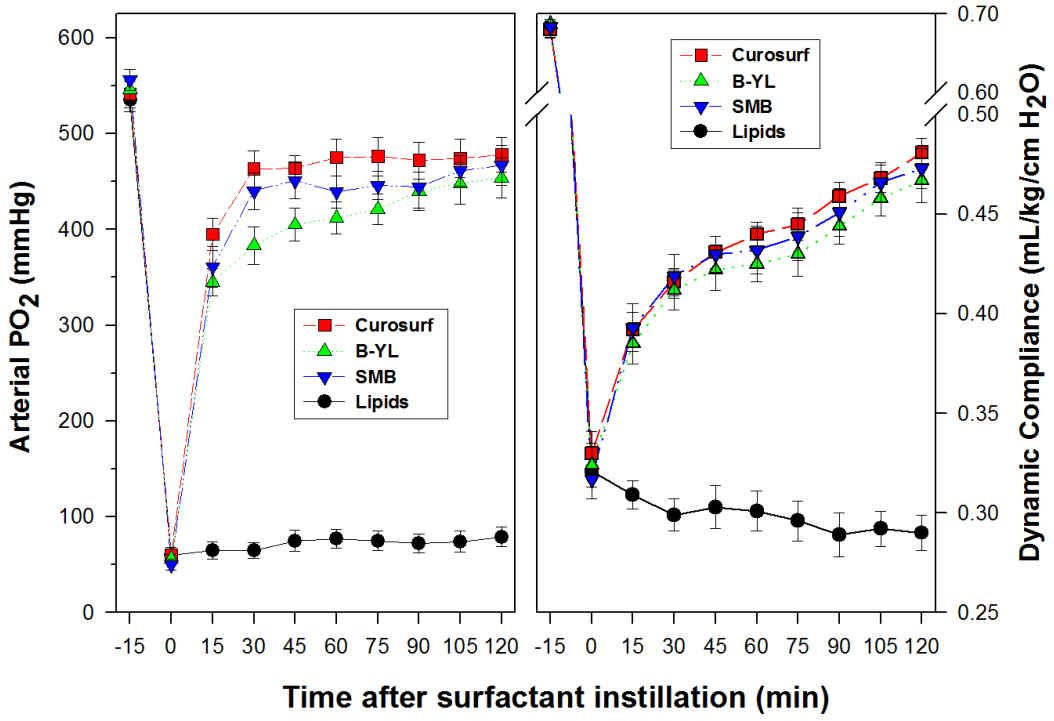

Figure 10. Arterial oxygenation and dynamic lung compliance in lavaged, surfactant-deficient, ventilated young adult rabbits treated with surfactant. Oxygenation (arterial PO_2 in mmHg) and dynamic lung compliance (mL/kg/cm H_2O) of 3% B-YL (n=9) and oxidized SMB (n=8) in surfactant lipids were compared with a clinical surfactant (Curosurf®) (n=8) or lipids alone (DPPC:POPC:POPG 5:3:2 mole:mole:mole) (n=8). Surfactant (100 mg/kg) was administered intratracheally as a bolus at time 0. Values are mean ± SEM. Differences in oxygenation and dynamic compliance between B-YL, SMB and Curosurf surfactants were not statistically significant, but differences with lipids alone were significant ($p<0.001$).

Discussion

The basic premise tested here was whether the 'sulfur-free' and 'oxidation-resistant' B-YL peptide, a 41-residue Super Mini-B (SMB) variant that has its four cysteine residues replaced by tyrosine and its two methionine residues replaced by leucine, would fold with the same α-helix hairpin conformation earlier shown by SMB to correlate with high *in vitro* and *in vivo* surfactant activities[8,10,14,17].

Circular dichroism (CD) and FTIR spectroscopy of 'B-YL' in surfactant lipids showed secondary structures compatible with the peptide folding as an α-helix hairpin, similar to that of SMB in lipids. All-atom (500 nsec) MD simulations confirmed that B-YL maintained its α-helix hairpin in a lipid bilayer, matching the hairpin obtained from the corresponding MD simulation of SMB. In contrast to the disulfide-reinforced helix-turn of SMB, however, the B-YL fold was stabilized by a core of clustered Tyr linking the N- and C-α-helices through noncovalent interactions involving "π-stacked" aromatic rings. MD simulations also indicated similar topological organizations for B-YL and SMB in the hydrated bilayers. Namely, the axes for the N- and C-α-helices of both peptides were nearly parallel to the membrane plane, and also the N-α-helix for both lies deeper in the bilayer subjacent to the lipid headgroup, while the C-α-helix binds to the more polar lipid-water interface. Captive bubble surfactometry indicated excellent surface activity for B-YL surfactant, while also showing good oxygenation and dynamic compliance in lavaged, surfactant-deficient adult rabbits, an animal model of acute lung injury (ALI) and acute respiratory distress syndrome (ARDS).

Our 'sulfur-free' and 'oxidation-resistant' B-YL mimic may therefore prove to be superior to its parent (oxidized) SMB for treating ALI/ARDS patients for several reasons. First, B-YL is less expensive and faster to synthesize than SMB because it omits an oxidation step and is self-folding. Second, the

substitution of Cys and Met residues with Tyr and Leu, respectively, may render the B-YL mimic less susceptible to the ROS inactivation typically observed in ALI/ARDS patients.

Lung immaturity and surfactant deficiency are the main cause of respiratory distress syndrome (RDS) in very preterm infants. Mechanical ventilation and exposure to high oxygen concentrations may lead to an inflammatory lung process resulting in bronchopulmonary dysplasia (BPD), a chronic lung disease of preterm infants. Use of antenatal steroids, administration of exogenous surfactant, and advanced modes of ventilation have shown only limited benefits in preventing RDS and BPD. In a neonatal rat model of hyperoxia-induced lung injury, we found that nebulized PPARγ agonist pioglitazone (PGZ) with B-YL surfactant accelerates lung maturation and prevents neonatal hyperoxia-induced lung injury more than with either modality alone, thereby potentially preventing BPD more effectively[58]. These findings suggest a potential role for B-YL surfactant as a vehicle for intrapulmonary drug therapy.

Conclusion

The 'sulfur-free' and 'oxidation-resistant' B-YL forms an amphipathic helix-hairpin in surfactant liposomes with high surface activity, and is functionally similar to its parent (oxidized SMB) and native SP-B. B-YL's resistance against free oxygen radical damage provides an extra edge over oxidized SMB in the treatment of respiratory failure in newborn infants with RDS and children and adults with ALI/ARDS.

Data availability

Raw data are available on OSF: http://doi.org/10.17605/OSF.IO/6295P[59]

Competing interests

No competing interests were disclosed.

Grant information

Bill and Melinda Gates Foundation [OPP1112090]. The funders had no role in study design, data collection and analysis, decision to publish, or preparation of the manuscript.

The funders had no role in study design, data collection and analysis, decision to publish, or preparation of the manuscript.

References

1. Veldhuizen R, Nag K, Orgeig S, *et al.*: **The role of lipids in pulmonary surfactant.** *Biochim Biophys Acta.* 1998; **1408**(2–3): 90–108.
PubMed Abstract | Publisher Full Text

2. Kahn MC, Anderson GJ, Anyan WR, *et al.*: **Phosphatidylcholine molecular species of calf lung surfactant.** *Am J Physiol.* 1995; **269**(5 Pt 1): L567–L573.
PubMed Abstract | Publisher Full Text

3. Notter RH, Wang Z, Egan EA, *et al.*: **Component-specific surface and physiological activity in bovine-derived lung surfactants.** *Chem Phys Lipids.* 2002; **114**(1): 21–34.
PubMed Abstract | Publisher Full Text

4. Nogee LM, Garnier G, Dietz HC, *et al.*: **A mutation in the surfactant protein B gene responsible for fatal neonatal respiratory disease in multiple kindreds.** *J Clin Invest.* 1994; **93**(4): 1860–1863.
PubMed Abstract | Publisher Full Text | Free Full Text

5. Clark JC, Wert SE, Bachurski CJ, *et al.*: **Targeted disruption of the surfactant protein B gene disrupts surfactant homeostasis, causing respiratory failure in newborn mice.** *Proc Natl Acad Sci USA.* 1995; **92**(17): 7794–7798.
PubMed Abstract | Free Full Text

6. Zaltash S, Palmblad M, Curstedt T, *et al.*: **Pulmonary surfactant protein B: a structural model and a functional analogue.** *Biochim Biophys Acta.* 2000; **1466**(1–2): 179–186.
PubMed Abstract | Publisher Full Text

7. Walther FJ, Gordon LM, Zasadzinski JA, *et al.*: **Surfactant protein B and C analogues.** *Mol Genet Metab.* 2000; **71**(1–2): 342–351.
PubMed Abstract | Publisher Full Text

8. Waring AJ, Walther FJ, Gordon LM, *et al.*: **The role of charged amphipathic helices in the structure and function of surfactant protein B.** *J Peptide Res.* 2005; **66**(6): 364–374.
PubMed Abstract | Publisher Full Text

9. Walther FJ, Waring AJ, Sherman MA, *et al.*: **Hydrophobic surfactant proteins and their analogues.** *Neonatology.* 2007; **91**(4): 303–310.
PubMed Abstract | Publisher Full Text

10. Walther FJ, Gordon LM, Waring AJ: **Design of surfactant protein B peptide mimics based on the saposin fold for synthetic lung surfactants.** *Biomed Hub.* 2016; **1**(3): pii: 451076.
PubMed Abstract | Publisher Full Text | Free Full Text

11. Johansson J, Jörnvall H, Curstedt T: **Human surfactant polypeptide SP-B. Disulfide bridges, C-terminal end, and peptide analysis of the airway form.** *FEBS Lett.* 1992; **301**(2): 165–167.
PubMed Abstract | Publisher Full Text

12. Munford RS, Sheppard PO, O'Hara PJ: **Saposin-like proteins (SAPLIP) carry out diverse functions on a common backbone structure.** *J Lipid Res.* 1995; **36**(8): 1653–1663.
PubMed Abstract

13. Bruhn H: **A short guided tour through functional and structural features of saposin-like proteins.** *Biochem J.* 2005; **389**(Pt 2): 249–257.
PubMed Abstract | Publisher Full Text | Free Full Text

14. Walther FJ, Waring AJ, Hernandez-Juviel JM, *et al.*: **Critical structural and functional roles for the N-terminal insertion sequence in surfactant protein B analogs.** *PLoS One.* 2010; **5**(1): e8672.
PubMed Abstract | Publisher Full Text | Free Full Text

15. Polin RA, Carlo WA; Committee on Fetus and Newborn, *et al.*: **Surfactant replacement therapy for preterm and term neonates with respiratory distress.** *Pediatrics.* 2014; **133**(1): 156–163.
PubMed Abstract | Publisher Full Text

16. Schwan AL, Singh SP, Davy JA, *et al.*: **Synthesis and activity of a novel diether phosphonoglycerol in phospholipase-resistant synthetic lipid:peptide lung surfactants().** *Medchemcomm* 2011; **2**(12): 1167–1173.
PubMed Abstract | Publisher Full Text | Free Full Text

17. Waring AJ, Gupta M, Gordon LM, *et al.*: **Stability of an amphipathic helix-hairpin surfactant peptide in liposomes.** *Biochim Biophys Acta.* 2016; **1858**(12): 3113–3119.
PubMed Abstract | Publisher Full Text | Free Full Text

18. Brower RG, Fessler HE: **Another "negative" trial of surfactant. Time to bury this idea?** *Am J Respir Crit Care Med.* 2011; **183**(8): 966–968.
PubMed Abstract | Publisher Full Text

19. Gunther A, Ruppert C, Schmidt R, *et al.*: **Surfactant alteration and replacement in acute respiratory distress syndrome.** *Respir Res.* 2001; **2**(6): 353–364.
PubMed Abstract | Publisher Full Text | Free Full Text

20. Lewis JF, Veldhuizen R: **The role of exogenous surfactant in the treatment of acute lung injury.** *Annu Rev Physiol.* 2003; **65**: 613–642.
PubMed Abstract | Publisher Full Text

21. Rodríguez-Capote K, Manzanares D, Haines T, *et al.*: **Reactive oxygen species inactivation of surfactant involves structural and functional alterations to surfactant proteins SP-B and SP-C.** *Biophys J.* 2006; **90**(8): 2808–2821.
PubMed Abstract | Publisher Full Text | Free Full Text

22. Manzanares D, Rodriguez-Capote K, Liu S, *et al.*: **Modification of tryptophan and methionine residues is implicated in the oxidative inactivation of surfactant protein B.** *Biochemistry.* 2007; **46**(18): 5604–5615.
PubMed Abstract | Publisher Full Text

23. Kim HI, Kim H, Shin YS, *et al.*: **Interfacial reactions of ozone with surfactant protein B in a model lung surfactant system.** *J Am Chem Soc.* 2010; **132**(7): 2254–2263.
PubMed Abstract | Publisher Full Text | Free Full Text

24. Hemming JM, Hughes BR, Rennie AR, *et al.*: **Environmental pollutant ozone causes damage to lung surfactant protein B (SP-B).** *Biochemistry.* 2015; **54**(33): 5185–5197.
PubMed Abstract | Publisher Full Text | Free Full Text

25. Sarker M, Rose J, McDonald M, *et al.*: **Modifications to surfactant protein B structure and lipid interactions under respiratory distress conditions: consequences of tryptophan oxidation.** *Biochemistry.* 2011; **50**(1): 25–36.
PubMed Abstract | Publisher Full Text

26. Baatz JE, Zou Y, Cox JT, *et al.*: **High-yield purification of lung surfactant proteins sp-b and sp-c and the effects on surface activity.** *Protein Expr Purif.* 2001; **23**(1): 180–190.
PubMed Abstract | Publisher Full Text

27. Johnson WC Jr: **Protein secondary structure and circular dichroism: a practical guide.** *Proteins.* 1990; **7**(3): 205–214.
PubMed Abstract | Publisher Full Text

28. Anthis NJ, Clore GM: **Sequence-specific determination of protein and peptide concentrations by absorbance at 205 nm.** *Protein Sci.* 2013; **22**(6): 851–858.
PubMed Abstract | Publisher Full Text | Free Full Text

29. Sreerama N, Venyaminov SY, Woody RW: **Estimation of the number of alpha-helical and beta-strand segments in proteins using circular dichroism spectroscopy.** *Protein Sci.* 1999; **8**(2): 370–380.
PubMed Abstract | Publisher Full Text | Free Full Text

30. Whitmore L, Wallace BA: **DICHROWEB, an online server for protein secondary structure analyses from circular dichroism spectroscopic data.** *Nucleic Acids Res.* 2004; **32**(Web Server Issue): W668–W673.
PubMed Abstract | Publisher Full Text | Free Full Text

31. Whitmore L, Wallace BA: **Protein secondary structure analyses from circular dichroism spectroscopy: methods and reference databases.** *Biopolymers.* 2008; **89**(5): 392–400.
PubMed Abstract | Publisher Full Text

32. Yamaguchi S, Hong T, Waring A, *et al.*: **Solid-state NMR investigations of peptide-lipid interaction and orientation of a beta-sheet antimicrobial peptide, protegrin.** *Biochemistry.* 2002; **41**(31): 9852–9862.
PubMed Abstract | Publisher Full Text

33. Kauppinen JK, Moffatt DJ, Mantsch HH, *et al.*: **Fourier self-deconvolution: A method for resolving intrinsically overlapped bands.** *Appl Spectr.* 1981; **35**(3): 271–276.
Publisher Full Text

34. Byler DM, Susi H: **Examination of the secondary structure of proteins by deconvolved FTIR spectra.** *Biopolymers.* 1986; **25**(3): 469–487.
PubMed Abstract | Publisher Full Text

35. Zhang Y: **I-TASSER server for protein 3D structure prediction.** *BMC Bioinformatics.* 2008; **9**: 40.
PubMed Abstract | Publisher Full Text | Free Full Text

36. Yang J, Yan R, Roy A, *et al.*: **The I-TASSER Suite: protein structure and function prediction.** *Nat Methods.* 2015; **12**(1): 7–8.
PubMed Abstract | Publisher Full Text | Free Full Text

37. Zhang Y, Skolnick J: **Scoring function for automated assessment of protein structure template quality.** *Proteins.* 2004; **57**(4): 702–710.
PubMed Abstract | Publisher Full Text

38. Lomize MA, Pogozheva ID, Joo H, *et al.*: **OPM database and PPM web server: resources for positioning of proteins in membranes.** *Nucleic Acids Res.* 2012; **40**(Database issue): D370–D376.
PubMed Abstract | Publisher Full Text | Free Full Text

39. Jo S, Kim T, Iyer VG, *et al.*: **CHARMM-GUI: a web-based graphical user interface for CHARMM.** *J Comput Chem.* 2008; **29**(11): 1859–1865.
PubMed Abstract | Publisher Full Text

40. Pronk S, Páll S, Schulz R, *et al.*: **GROMACS 4.5: a high-throughput and highly parallel open source molecular simulation toolkit.** *Bioinformatics.* 2013; **29**(7): 845–854.
PubMed Abstract | Publisher Full Text | Free Full Text

41. Snider C, Jayasinghe S, Hristova K, *et al.*: **MPEx: a tool for exploring membrane proteins.** *Protein Sci.* 2009; **18**(12): 2624–2628.
PubMed Abstract | Publisher Full Text | Free Full Text

42. Jayasinghe S, Hristova K, White SH: **Energetics, stability, and prediction of transmembrane helices.** *J Mol Biol.* 2001; **312**(5): 927–934.
PubMed Abstract | Publisher Full Text

43. Walther FJ, Waring AJ, Hernández-Juviel JM, *et al.*: **Surfactant protein C peptides with salt-bridges ("ion-locks") promote high surfactant activities by mimicking the α-helix and membrane topography of the native protein.** *PeerJ.* 2014; **2**: e485.
PubMed Abstract | Publisher Full Text | Free Full Text

44. Wimley WC, Creamer TP, White SH: **Solvation energies of amino acid side chains and backbone in a family of host-guest pentapeptides.** *Biochemistry.* 1996; **35**(16): 5109–5124.
PubMed Abstract | Publisher Full Text

45. Schürch S, Bachofen H, Goerke J, *et al.*: **A captive bubble method reproduces the in situ behavior of lung surfactant monolayers.** *J Appl Physiol (1985).* 1989; **67**(6): 2389–2396.
PubMed Abstract | Publisher Full Text

46. Schürch S, Bachofen H, Possmayer F: **Surface activity *in situ*, *in vivo*, and in the captive bubble surfactometer.** *Comp Biochem Physiol A Mol Integr Physiol.* 2001; **129**(1): 195–207.
PubMed Abstract | Publisher Full Text

47. Surewicz WK, Mantsch HH: **New insight into protein secondary structure from resolution-enhanced infrared spectra.** *Biochim Biophys Acta.* 1988; **952**(2): 115–130.
PubMed Abstract | Publisher Full Text

48. Chen YH, Yang JT, Chau KH: **Determination of the helix and beta form of proteins in aqueous solution by circular dichroism.** *Biochemistry.* 1974; **13**(16): 3350–3359.
PubMed Abstract | Publisher Full Text

49. Gordon LM, Horvath S, Longo ML, *et al.*: **Conformation and molecular topography of the N-terminal segment of surfactant protein B in structure-promoting environments.** *Protein Sci.* 1996; **5**(8): 1662–1675.
PubMed Abstract | Publisher Full Text | Free Full Text

50. Ou X, Zheng W, Shan Y, *et al.*: **Identification of the Fusion Peptide-Containing Region in Betacoronavirus Spike Glycoproteins.** *J Virol.* 2016; **90**(12): 5586–5600.
PubMed Abstract | Publisher Full Text | Free Full Text

51. Zhang Y, Skolnick J: **TM-align: a protein structure alignment algorithm based on the TM-score.** *Nucleic Acids Res.* 2005; **33**(7): 2302–2309.
PubMed Abstract | Publisher Full Text | Free Full Text

52. Engelman DM, Steitz TA: **The spontaneous insertion of proteins into and across membranes: the helical hairpin hypothesis.** *Cell.* 1981; **23**(2): 411–422.
PubMed Abstract | Publisher Full Text

53. Thayer MM, Ahern H, Xing D, *et al.*: **Novel DNA binding motifs in the DNA repair enzyme endonuclease III crystal structure.** *EMBO J.* 1995; **14**(16): 4108–4120.
PubMed Abstract | Free Full Text

54. Kim JH, Hartley TL, Curran AR, *et al.*: **Molecular dynamics studies of the transmembrane domain of gp41 from HIV-1.** *Biochim Biophys Acta.* 2009; **1788**(9): 1804–1812.
PubMed Abstract | Publisher Full Text | Free Full Text

55. Waters ML: **Aromatic interactions in model systems.** *Curr Opin Chem Biol.* 2002; **6**(6): 736–741.
PubMed Abstract | Publisher Full Text

56. Wheeler SE, Bloom JW: **Toward a more complete understanding of noncovalent interactions involving aromatic rings.** *J Phys Chem A.* 2014; **118**(32): 6133–6147.
PubMed Abstract | Publisher Full Text

57. McGaughey GB, Gagné M, Rappé AK: **pi-Stacking interactions. Alive and well in proteins.** *J Biol Chem.* 1998; **273**(25): 15458–15463.
PubMed Abstract | Publisher Full Text

58. Sakurai R, Lee C, Shen H, *et al.*: **A Combination of the Aerosolized PPAR-γ Agonist Pioglitazone and a Synthetic Surfactant Protein B Peptide Mimic Prevents Hyperoxia-Induced Neonatal Lung Injury in Rats.** *Neonatology.* 2018; **113**(4): 296–304. in press.
PubMed Abstract | Publisher Full Text

59. Walther FJ: **B-YL Data.** *Open Science Framework.* 2018.
Data Source

Open Peer Review

Current Peer Review Status: ✗ ?

Version 1

Reviewer Report 28 March 2018

https://doi.org/10.21956/gatesopenres.13861.r26281

?

Jesús Pérez-Gil
Department of Biochemistry, Faculty of Biology and Research Institute Hospital 12 de Octubre, Complutense University, Madrid, Spain

This study summarizes data on the design, synthesis, structure, lipid-protein interactions and surface activity -in vitro and in vivo- of a synthetic peptide analog that mimics certain functional segments of pulmonary surfactant protein SP-B. The team responsible has a large expertise in the design and optimization of this type of peptide mimics of surfactant proteins, and the current work is a natural and smart extension of previous work.

In the current study, an analog to a well-know synthetic surrogate of SP-B, the so-called “mini-B”, has been produced and analyzed in detail. This ‘B-YL’ peptide is a mini-B version in which cysteines forming disulphide bonds, in both wild-type SP-B ad mini-B, have been substituted by tyrosines. The rational is that tyrosines could also contribute to stabilize peptide-peptide interactions via pi-stacking and so yielding the typical alpha-helical hairpin bridging N-terminal and C-terminal helical segments of SP-B together. The substitution of Cys by Tyr would on the other hand supposedly render a peptide surrogate with lower propensity to oxidation, according to the authors, thanks to the elimination of cysteine residues. The authors essentially conclude that the B-YL analog is entirely comparable, structurally and functionally, to the mini-B construct, and therefore that it would be equally useful to produce synthetic surfactants for therapeutic applications.

In general term, the experiments have been properly carried out, and they provide extensive proofs that the peptide behaves “in general terms” as it was expected. In this sense, it is interesting to see how the substitution of two disulphides by tyrosine clustering could also serve as a basis to build a membrane active peptide fold such as the one of miniB. This is certainly an advantage from the point of view of its synthesis and production. It would be for instance a large advantage to produce inexpensive large amounts of this type of peptides by overexpression in bacteria, where formation of disulphides would certainly be a limitation.

What I am not so sure is whether this peptide would actually be less susceptible to oxidation, and whether this peptide is actually a good mimic of SP-B, or at least as good as miniB.

As mentioned by the authors, one of the targets of oxidation-promoted inactivation of surfactant proteins are the aromatic residues. Actually, oxidation of the single tryptophan of SP-B (as shown by the group of Possmayer), located at its N-terminal helical segment, is associated with complete inactivation of the protein. It had been previously demonstrated (see for instance Ryan et al.(2005) [1] or Serrano et al.(2006)[2]) that this tryptophan is essential at the N-terminal end of SP-B, because it takes part of a highly hydrophobic-at-interface segment which defines very high affinity for insertion into amphipathic environments such as the air-liquid interface. Now this tryptophan has been substituted in the whole peptide by 4 tyrosines. Tyrosines may maintain a high affinity for the interface, but at the cost of being also highly susceptible to oxidation. The authors could have shown if it is true that exposure of B-YL to oxidant reactions preserve its activity better than in the case of mini-B.

Another major problem in my opinion of the substitution of disulphides by aromatic residues is that it may change dramatically the way the peptide perturb surfactant membranes and films, which is crucial for a good surface activity. Disulphides surely impose a very strong constraint to the way the two helical segments orientate into the membrane. As a matter of fact, the tilting of the amphipathic N-terminal and C-terminal helical segments of SP-B, which is crucial for perturbing lipid packing to the point of facilitating the transfer of surface active lipid molecules between different bilayers or between the bilayers and the interfacial film, may be subtly different in the case of miniB, and even more in the B-YL analog. I may agree that tyrosine clustering could roughly join the C-terminal and N-terminal segments together, but they would do that in a much more flexible, dynamic and fluctuating way than the disulphides, and that may reduce the efficiency for the protein to induce membrane perturbation. This could be the reason why the maximum surface tension during cycling of lipid-peptide films at the CBS is higher in the case of B-YL than in mini-B, and much more than in the case of Curosurf containing true SP-B, where the full protein structure may impose a much more defined geometry to the N-terminal/C-terminal helical cluster. The limited MD simulations in the presence of lipids also seem to show differences in tilting of the helical segments with respect to the lipid surface. The authors have neglected these differences, but it would be important to show if they do really exist and whether they are reproducible.

Other problem related with the final geometry of the lipid-protein complexes comes from the high hydrophobicity-at interface of the aromatic residues. The introduction of the 4 tyrosines may force a orientation of the mini-B construct which is much more anchored to the surface of the membrane, where aromatic residues tend to partitition, than it is the case for the tyrosine-free miniB analog.

The authors may argue that the MD simulations do not reflect substantial differences in this respect, but a 500 nsec simulation may or may not be enough to get the fully equilibrated state. Have the authors data to evaluate whether longer simulation times could reflect further differences?

There is an additional important issue that may arise from the substitution of disulphides by tyrosines that in my opinion has not been properly addressed. If tyrosine clustering is enough to sustain intramolecular peptide-peptide interactions stabilizing the miniB hairpin, it may also sustain intermolecular peptide-peptide interactions, which could end in peptide aggregation and clustering, potentially reducing lipid dispersion and surface activity. The simulations run do not

contain multiple copies of the peptide, which could assess whether intramolecular interactions are or not preferred over intermolecular interactions, provided that long enough simulation times are applied. This problem does not exist, obviously, when the intramolecular interactions are maintained through covalent disulphide bonds.

Other questions that would require some discussion include:

The use of surfactant therapy on therapies to treat ALI and ARDS is under strong debate. It is doubtful that a simple synthetic surfactant such as those containing mini-B-like peptides as surrogates of SP-B would be ever useful to treat ARDS patients.

The way captive bubble experiments have been performed has been poorly explained and produce some confusion. In page 6, it is stated that CBS has been operated at “physiological cycling rate”. However, in page 14, it is stated that “Surface activity of … were consistently and equally low during quasi-static cycling…” What has been the compression-expansion cycling rate used? There is also some confusion with respect to the concentration at which the different surfactants have been tested in the CBS. In page 6, it is stated that “We routinely analyze surfactant preparations at an average surfactant lipid concentration of 25 microgram/mL”. Later it is stated that “We used a B-YL surfactant mixture consisting on… with a concentration of 35 mg/mL”. Could you, please, clarify what is the lipid concentration used to obtain each of the CBS isotherms? How this concentration is applied (in the bulk hypophase in which the bubble is formed, or directly at the air-water interface)?

The results of MD simulations have been taken as a proof that the cys-by-tyr substitutions can also sustain the intramolecular peptide-peptide interactions defining the formation of the miniB-like helical hairpin in surfactant lipids. The question is what were the initial points of at which those simulations were started? Where the aromatic sidechains already clustered or where the peptides initially embedded into the membranes in an extended conformation, to see whether the propensity for the hairpin to be formed could be entirely sustained by the affinity of tyrosines to pile? This second type of experiments could be crucial. Even better if the simulation cell could contain not one but several copies of the peptides.

The experiments in vivo seems to indicate that the B-YL analog is less active than miniB or Curosurf to produce good oxygenation indexes, at least at the shortest times. The authors state that there is no statistical difference between the activity in vivo of the two different analogs. Have they tested statistical significance of the means only at the end times or have they checked whether differences at shorter times could indicate that there may be a significant difference in kinetics (which can also functionally important)?

In summary, I think the study can be of interest for the scientists in the field, and may open alternatives in the design of other peptides or proteins potentially mimicking the structure-function determinants of surfactant proteins. However, instead of merely summarizing the main parallelisms found, the Discussion should be completed by addressing all the questions raised in this report, which could add substantially to the structural and functional features that may be important to test when designing future new peptide surfactant additives for therapeutic purposes.

References
1. Ryan MA, Qi X, Serrano AG, Ikegami M, et al.: Mapping and analysis of the lytic and fusogenic domains of surfactant protein B.*Biochemistry*. 2005; **44** (3): 861-72 PubMed Abstract | Publisher Full Text
2. Serrano AG, Ryan M, Weaver TE, Pérez-Gil J: Critical structure-function determinants within the N-terminal region of pulmonary surfactant protein SP-B.*Biophys J*. 2006; **90** (1): 238-49 PubMed Abstract | Publisher Full Text

Is the work clearly and accurately presented and does it cite the current literature?
Partly

Is the study design appropriate and is the work technically sound?
Yes

Are sufficient details of methods and analysis provided to allow replication by others?
Partly

If applicable, is the statistical analysis and its interpretation appropriate?
Partly

Are all the source data underlying the results available to ensure full reproducibility?
Partly

Are the conclusions drawn adequately supported by the results?
Partly

Competing Interests: No competing interests were disclosed.

I confirm that I have read this submission and believe that I have an appropriate level of expertise to confirm that it is of an acceptable scientific standard, however I have significant reservations, as outlined above.

Author Response 04 Jul 2018

Frans Walther, Los Angeles Biomedical Research Institute at Harbor-UCLA Medical Center, Torrance, USA

Response to Reviewer Dr. Pérez-Gil:

1. What I am not so sure is whether this peptide would actually be less susceptible to oxidation, and whether this peptide is actually a good mimic of SP-B, or at least as good as miniB.

As mentioned by the authors, one of the targets of oxidation-promoted inactivation of surfactant proteins are the aromatic residues. Actually, oxidation of the single tryptophan of SP-B (as shown by the group of Possmayer), located at its N-terminal helical segment, is associated with complete inactivation of the protein. It had been previously demonstrated

(see for instance Ryan et al.(2005)[1] or Serrano et al.(2006)[2]) that this tryptophan is essential at the N-terminal end of SP-B, because it takes part of a highly hydrophobic-at-interface segment which defines very high affinity for insertion into amphipathic environments such as the air-liquid interface. Now this tryptophan has been substituted in the whole peptide by 4 tyrosines. Tyrosines may maintain a high affinity for the interface, but at the cost of being also highly susceptible to oxidation. The authors could have shown if it is true that exposure of B-YL to oxidant reactions preserve its activity better than in the case of mini-B.

Response: As suggested by the other reviewer, Dr. Valerie Booth, we decided to remove all claims of “oxidation-resistance” in the title, abstract, conclusion and other parts of the text. The B-YL peptide is somewhat less sensitive to oxidation by Leu substitution for Met and storage for one year showed no Tyrosine or Tryptophan oxidation by mass spec. B-YL is actually as good a mimic of SP-B as Super Mini-B at captive bubble surfactometry and in the lavaged, surfactant-deficient rabbits.

2. Another major problem in my opinion of the substitution of disulphides by aromatic residues is that it may change dramatically the way the peptide perturb surfactant membranes and films, which is crucial for a good surface activity. Disulphides surely impose a very strong constraint to the way the two helical segments orientate into the membrane. As a matter of fact, the tilting of the amphipathic N-terminal and C-terminal helical segments of SP-B, which is crucial for perturbing lipid packing to the point of facilitating the transfer of surface active lipid molecules between different bilayers or between the bilayers and the interfacial film, may be subtly different in the case of miniB, and even more in the B-YL analog. I may agree that tyrosine clustering could roughly join the C-terminal and N-terminal segments together, but they would do that in a much more flexible, dynamic and fluctuating way than the disulphides, and that may reduce the efficiency for the protein to induce membrane perturbation. This could be the reason why the maximum surface tension during cycling of lipid-peptide films at the CBS is higher in the case of B-YL than in mini-B, and much more than in the case of Curosurf® containing true SP-B, where the full protein structure may impose a much more defined geometry to the N-terminal/C-terminal helical cluster. The limited MD simulations in the presence of lipids also seem to show differences in tilting of the helical segments with respect to the lipid surface. The authors have neglected these differences, but it would be important to show if they do really exist and whether they are reproducible.

Other problem related with the final geometry of the lipid-protein complexes comes from the high hydrophobicity-at interface of the aromatic residues. The introduction of the 4 tyrosines may force a orientation of the mini-B construct which is much more anchored to the surface of the membrane, where aromatic residues tend to partitition, than it is the case for the tyrosine-free miniB analog.

Response: Simulations show no difference in surface orientation. However, we decided to remove the homology models, molecular dynamic (MD) simulation and Membrane Protein Explorer (MPEx) from the manuscript as modeling was only a secondary focus and we plan to publish a more extensive data set in a follow-up paper.

3. The authors may argue that the MD simulations do not reflect substantial differences in

this respect, but a 500 nsec simulation may or may not be enough to get the fully equilibrated state. Have the authors data to evaluate whether longer simulation times could reflect further differences?

Response: We extended simulations to one microsecond. However, we have decided to remove the homology models, molecular dynamic (MD) simulation and Membrane Protein Explorer (MPEx) from the manuscript as modeling was only a secondary focus and we plan to publish a more extensive data set in a follow-up paper.

4. There is an additional important issue that may arise from the substitution of disulphides by tyrosines that in my opinion has not been properly addressed. If tyrosine clustering is enough to sustain intramolecular peptide-peptide interactions stabilizing the miniB hairpin, it may also sustain intermolecular peptide-peptide interactions, which could end in peptide aggregation and clustering, potentially reducing lipid dispersion and surface activity. The simulations run do not contain multiple copies of the peptide, which could assess whether intramolecular interactions are or not preferred over intermolecular interactions, provided that long enough simulation times are applied. This problem does not exist, obviously, when the intramolecular interactions are maintained through covalent disulphide bonds.

Response: Insertion sequence keeps this from happening. However, we decided to remove the homology models, molecular dynamic (MD) simulation and Membrane Protein Explorer (MPEx) paragraphs from the manuscript as modeling was only a secondary focus and plan to publish a more extensive data set in a follow-up paper.

5. The use of surfactant therapy on therapies to treat ALI and ARDS is under strong debate. It is doubtful that a simple synthetic surfactant such as those containing mini-B-like peptides as surrogates of SP-B would be ever useful to treat ARDS patients.

Response: We agree with the reviewer and removed the statements about surfactant therapy for ALI/ARDS from the abstract, the last paragraph of page 3, discussion and conclusion.

6. The way captive bubble experiments have been performed has been poorly explained and produce some confusion. In page 6, it is stated that CBS has been operated at “physiological cycling rate”. However, in page 14, it is stated that “Surface activity of … were consistently and equally low during quasi-static cycling…” What has been the compression-expansion cycling rate used? There is also some confusion with respect to the concentration at which the different surfactants have been tested in the CBS. In page 6, it is stated that “We routinely analyze surfactant preparations at an average surfactant lipid concentration of 25 microgram/mL”. Later it is stated that “We used a B-YL surfactant mixture consisting on… with a concentration of 35 mg/mL”. Could you, please, clarify what is the lipid concentration used to obtain each of the CBS isotherms? How this concentration is applied (in the bulk hypophase in which the bubble is formed, or directly at the air-water interface)?

Response: We actually do both quasi-static and dynamic cycling on the CBS. Quasi-static compression and expansion of the air bubble is performed in discrete steps at a rate of 5%

of the bubble volume every 10 sec with continuous video recording of the bubble shape. Dynamic compression and expansion cycling is performed between 10 and 110% of the original bubble area at a cycling rate of 20 cycles/min. Both modalities show extreme flattening of the bubble in active surfactant preparations. In figure 9 we present the data from quasi-static cycling. We routinely analyze surfactant preparations at an average surfactant lipid concentration of 25 µg/mL in the bubble chamber, but as Curosurf® is more concentrated than synthetic surfactant, we applied 1 µL of synthetic surfactant at 35 mg/mL and 0.5 µL of Curosurf® at 80 mg/mL to the bubble chamber (1.5 mL volume). After introducing surfactant and the air bubble into the CBS chamber, both move upwards to the interface with the agarose plug. This information was added to the methods section.

7. The results of MD simulations have been taken as a proof that the cys-by-tyr substitutions can also sustain the intramolecular peptide-peptide interactions defining the formation of the miniB-like helical hairpin in surfactant lipids. The question is what were the initial points of at which those simulations were started? Where the aromatic sidechains already clustered or where the peptides initially embedded into the membranes in an extended conformation, to see whether the propensity for the hairpin to be formed could be entirely sustained by the affinity of tyrosines to pile? This second type of experiments could be crucial. Even better if the simulation cell could contain not one but several copies of the peptides.

Response: See above, we decided to remove the homology models, molecular dynamic (MD) simulation and Membrane Protein Explorer (MPEx) from the manuscript as modeling was only a secondary focus and we plan to publish a more extensive data set in a follow-up paper.

8. The experiments in vivo seems to indicate that the B-YL analog is less active than miniB or Curosurf to produce good oxygenation indexes, at least at the shortest times. The authors state that there is no statistical difference between the activity in vivo of the two different analogs. Have they tested statistical significance of the means only at the end times or have they checked whether differences at shorter times could indicate that there may be a significant difference in kinetics (which can also functionally important)?

Response: In response to the reviewer, we calculated the statistical significance of differences in means at every 15 min time-point after surfactant instillation and found no significant differences in dynamic compliance for the 3 surface-active surfactant preparations throughout the experiments. During the first 75 min after surfactant administration, mean oxygenation values of the B-YL surfactant group were slightly lower than in the Curosurf® group ($p<0.03$), but not different from those in the Super Mini-B (SMB) group, suggesting initial differences in kinetics. Thereafter oxygenation was similar in B-YL, SMB and Curosurf® surfactants. This info was added to the results section.

Competing Interests: No competing interests were disclosed.

Reviewer Report 20 March 2018

https://doi.org/10.21956/gatesopenres.13861.r26299

Valerie Booth
Department of Biochemistry , Memorial University of Newfoundland, St. John's, NL, Canada

Walther, Gupta, Gordon and Waring present studies of a peptide called “B-YL” which they propose may be of utility as a component of exogenous lung surfactant replacement therapy for conditions such as ARDS and ALI. In these conditions, the lung environment is “hostile” to lung surfactant proteins and a variety of inactivating components including reactive oxygen species are present. The experimental work is comprehensive and complementary, as well as expertly done and clearly described (with a few exceptions as detailed below). I appreciate the effort to include the *in vitro* and *in vivo* functional work, as well as the structural studies. I also believe that the general thrust of the work – creating peptide components that can act in place of full length lung surfactant proteins – is very worthwhile.

However, I do have trouble with the premise for the paper – that removing the cysteines and methionines will make the peptide “oxidation-resistant”. The authors present no justification that cysteines are a target of ROS damage. In the lung surfactant literature, it’s been shown that tryptophan 9 is the main target of oxidation, with methionine residues as a secondary target[1]. The peptide B-YL leaves this critical tryptophan unchanged and so may well be just as susceptible to damage as the parent peptide, super Mini-B. Furthermore, it’s been proposed that one of the roles of methionines may be to protect the tryptophan by competing for ROS. So, removing the methionines may actually make the protein MORE susceptible to damage. Thus, I think the options are to either back up the assertion that the new peptide is “oxidation-resistant” with convincing experiments or references OR to remove all claims of “oxidation-resistant” from the title, abstract, conclusion and other parts of the text. I think the work stands up perfectly well without the oxidation-resistant angle, because as the authors point out, the removal of the cysteines makes it more feasible to scale up production to the scale needed for clinical work.

Here are the rest of my comments, roughly in the same order as the manuscript:

1. Page 3 bottom left. Could you add a sentence to describe what an alpha-helix hairpin is. It’s referred to several times later on so it would be good to start with a clear picture of what it is.

2. Page 3, right hand column, 15 lines from the bottom reads “Trp-9 plays a role in the diminished surface activity possibly due to fraying of the N-terminal alpha-helix 24,25”. Reference 25 actually suggests the activity may be changed because the oxidizing Trp to kynurenine causes the peptide to change its depth within the lipid layer.

3. Page 3, right hand column, 1st sentence of the last paragraph. I’m not sure we can say that “ALI/ARDS… REQUIRES the use of exogenous surfactants” since I’m not sure that it’s ever been convincingly shown that exogenous surfactant treatment substantially helps patients with ALI/ARDS – can you re-phrase or back-up this statement.

4. Page 3, last sentence. It would be good to explain why tyrosine (instead of some other amino acid) was chosen to replace the Cys and Met.

5. Methods paragraph 2 and throughout. It is very (very!) confusing that Super Mini-B is referred to throughout as “oxidized” SMB. The “oxidation” is just the normal formation of disulfide bonds and since the paper is supposedly about making a “oxidation-resistant” version of SMB the two meanings are bound to be confounded by readers. I would just call it “SMB with disulfides” or something else along those lines.

6. Page 5, last paragraph. Instead of referring to a “recent homology modeling program” and then naming the actual program 5 lines later, I would put the name of the program right into this first sentence.

7. Page 5, last paragraph – which pdb files went into the homology model? I think it’s important to know this as there’s not that much sequence homology between SP-B and known structures so whichever ones I-TASSER is choosing will have a big influence on how the structures look.

8. Page 5 under the MD section… what was the initial position of the peptide within the bilayer and how did it change during the simulation? Note that Khatami et al.[2] found that the secondary structure of full length SP-B in MD simulations varied a lot with the position with respect to the bilayer. This is probably less important for the smaller peptide, but is still worth mentioning the initial position and the rationale for it.

9. Page 6 under Captive bubble surfactometry. I’m guessing 3% of B-YL peptide is by mole? Can you add this info (here and later on) so we’re clear?

10. Page 7 top left. At some point (not necessarily here) it would be good to compare the dose of surfactant (in mg/kg body weight) to what is given to preemies. Also could you comment on why the dose is lower for Curosurf than for SMB?

11. Page 7. First paragraph under results and Table 1. I’m not sure its appropriate to quote “Beta-sheet” content since I don’t think you are proposing there is an actual sheet involved. Could you choose something more appropriate, like “beta-strand” or “beta-hairpin” or just “beta-structure”.

12. Figure 3. Since estimating secondary structure is so dependent on protein concentration, it would be good to know what method was used to determine the peptide concentration (desalted dry weight, UV, colorimeteric assay ?).

13. Page 10, and later. The “core of hydrophobic residues” should be compared to that of Mini-B’s experimental structure. How much of this core is preserved in your predictions for the SMB and B-YL structures?

14. Page 10, bottom left and elsewhere. Can you replace all instances of “largely agrees with” with something more quantitative – like backbone RMSD.

15. Page 11, left hand column. In addition to the pi stacking interactions, I’m wondering what

the hydroxyl on the tyrosines are doing – are they finding anything to hydrogen bond to? What?

16. Page 11, 2nd sentence of the 2nd paragraph: as for 14 above, please replace “generally in good agreement” with something more precise.

17. Page 11 – How do the starting and final structures and hydrophobic core compare to the experimental structure for Mini-B in SDS micelles?

18. Page 14 – right hand side, please replace “good overlap” and “remarkably analogous” with something more precise like RMSD.

References

1. Manzanares D, Rodriguez-Capote K, Liu S, Haines T, et al.: Modification of tryptophan and methionine residues is implicated in the oxidative inactivation of surfactant protein B.*Biochemistry*. 2007; **46** (18): 5604-15 PubMed Abstract | Publisher Full Text
2. Khatami MH, Saika-Voivod I, Booth V: All-atom molecular dynamics simulations of lung surfactant protein B: Structural features of SP-B promote lipid reorganization.*Biochim Biophys Acta*. **1858** (12): 3082-3092 PubMed Abstract | Publisher Full Text

Is the work clearly and accurately presented and does it cite the current literature?
Partly

Is the study design appropriate and is the work technically sound?
Partly

Are sufficient details of methods and analysis provided to allow replication by others?
Yes

If applicable, is the statistical analysis and its interpretation appropriate?
Yes

Are all the source data underlying the results available to ensure full reproducibility?
No

Are the conclusions drawn adequately supported by the results?
Partly

Competing Interests: No competing interests were disclosed.

I confirm that I have read this submission and believe that I have an appropriate level of expertise to state that I do not consider it to be of an acceptable scientific standard, for reasons outlined above.

Author Response 04 Jul 2018

Frans Walther, Los Angeles Biomedical Research Institute at Harbor-UCLA Medical Center, Torrance, USA

Response to Reviewer Dr. Valerie Booth:

General response

Suggestion to remove all claims of "oxidation-resistance" from the title, abstract, conclusion, and other parts of the text.

Response: We removed all claims of "oxidation-resistance" from the title, abstract, conclusion, and text. As B-YL peptide is sulfur-free, the title was changed to: "A sulfur-free peptide mimic of surfactant protein B (B-YL) exhibits high in vitro and in vivo surface activities".

Specific comments:
1. Page 3, bottom left. Could you add a sentence to describe what an alpha-helix hairpin is. It's referred to several times later on so it would be good to start with a clear picture of what it is.

Response: We have added to Page 3 bottom left a definition of an alpha helix hairpin structure as well as provided a literature reference for it: "SMB incorporates the N-terminal α-helix (~residues 8-25) and C-terminal α-helix (~residues 63-78) of native SP-B as a single linear peptide (Figure 1A), joined together with a customized turn to form a α-helix hairpin (a-helix/turn/a-helix, ata) [Fezoui Y et al., 1994]."

2. Page 3, right hand column, 15 lines from the bottom reads "Trp-9 plays a role in diminished surface activity possibly due to fraying of the N-terminal alpha helix 24-25". Reference 25 actually suggest the activity may be changed because the oxidizing Trp to kynurenine causes the peptide to change its depth within the lipid layer.

Response: We have added here that this is in the full-length protein and in addition we have incorporated mass spec findings in the results section that indicate that the B-YL peptide does not undergo oxidation of its aromatic amino acids when stored in surfactant lipids for one year:
"Trp-9 can play a role in diminished surface activity in the full length native protein possibly due to fraying of the N-terminal alpha helix 24-25".
"Mass spectral analysis of the B-YL peptide indicated there was no change in the molecular weight due to oxidation of tyrosines or tryptophan for one year when formulated with surfactant lipids."

3. Page 3, right hand column, 1st sentence of the last paragraph. I'm not sure we can say that "ALI/ARDS… REQUIRES the use of exogenous surfactants" since I'm not sure that it's ever been convincingly shown that exogenous surfactant treatment substantially helps patients with ALI/ARDS – can you re-phrase or back-up this statement.

Response: We agree with the reviewer and removed this sentence and “surfactant dysfunction in ALI/ARDS” in the next sentence.

4. Page 3, last sentence. It would be good to explain why tyrosine (instead of some other amino acid) was chosen to replace the Cys and Met.

Response: We have added an additional sentence (line 2, page 4) to explain our rational in the selection of tyrosine and leu for cysteine and methionine. We opted for leucine rather than the commonly used norleucine because we felt that the use of non-natural amino acids may cause longer term metabolic problems *in vivo*.
“Tyrosine was substituted for cysteine because of its aromatic ring interactions that emulate disulfide formation [55, 56, 57] and methionine, that is easily oxidized, was replaced by leucine based on its similar molecular structure and polarity [44].”

5. Methods paragraph 2 and throughout. It is very (very!) confusing that Super Mini-B is referred to throughout as “oxidized” SMB. The “oxidation” is just the normal formation of disulfide bonds and since the paper is supposedly about making a “oxidation-resistant” version of SMB the two meanings are bound to be confounded by readers. I would just call it “SMB with disulfides” or something else along those lines.

Response: We have modified the text using “SMB” instead of “oxidized SMB” in accordance with the reviewer’s comments, so that there is no confusion with oxidation of the peptide per se.

6. Page 5, last paragraph. Instead of referring to a “recent homology modeling program” and then naming the actual program 5 lines later, I would put the name of the program right into this first sentence.

Response: We decided to remove the homology models, molecular dynamic (MD) simulation and Membrane Protein Explorer (MPEx) from the manuscript as modeling was only a secondary focus and we plan to publish a more extensive data set in a follow-up paper.

7. Page 5, last paragraph – which pdb files went into the homology model? I think it’s important to know this as there’s not that much sequence homology between SP-B and known structures so whichever ones I-TASSER is choosing will have a big influence on how the structures look.

Response: Please see our response to reviewer’s comment #6.

8. Page 5 under the MD section… what was the initial position of the peptide within the bilayer and how did it change during the simulation? Note that Khatami et al.[2] found that the secondary structure of full length SP-B in MD simulations varied a lot with the position with respect to the bilayer. This is probably less important for the smaller peptide, but is still worth mentioning the initial position and the rationale for it.

Response: Please see our response to reviewer’s comment #6.

9. Page 6 under Captive bubble surfactometry. I'm guessing 3% of B-YL peptide is by mole? Can you add this info (here and later on) so we're clear?

Response: We used 3 mole % of B-YL or SMB peptide. We have clarified the concentration by including a reference [17] detailing the formulation used for SMB and B-YL peptides.

10. Page 7 top left. At some point (not necessarily here) it would be good to compare the dose of surfactant (in mg/kg body weight) to what is given to preemies. Also could you comment on why the dose is lower for Curosurf than for SMB?

Response: All animals received 100 mg lipids/kg bodyweight of one of the 4 surfactant preparations. The clinical surfactant Curosurf® is formulated by the manufacturer at 80 mg/mL and SMB and B-YL surfactant and lipids alone were formulated at 35 mg/mL, so Curosurf® was dosed at 1.25 mL/kg and the synthetic surfactants at 2.9 mL/kg. Clinical surfactant is routinely dosed at 100 mg/kg in premature infants with RDS, so the dosages used here were similar to those used clinically. This info was added to the methods on page 7.

11. Page 7. First paragraph under results and Table 1. I'm not sure its appropriate to quote "Beta-sheet" content since I don't think you are proposing there is an actual sheet involved. Could you choose something more appropriate, like "beta-strand" or "beta-hairpin" or just "beta-structure".

Response: We have replaced "Beta-sheet" with "beta-structure".

12. Figure 3. Since estimating secondary structure is so dependent on protein concentration, it would be good to know what method was used to determine the peptide concentration (desalted dry weight, UV, colorimeteric assay ?).

Response: We have added the following description and reference with regard to peptide quantitation: "Peptides were routinely quantitated using UV absorbance based on the assay procedure developed by Anthis and Clore (Protein Science, 2013)".

13. Page 10, and later. The "core of hydrophobic residues" should be compared to that of Mini-B's experimental structure. How much of this core is preserved in your predictions for the SMB and B-YL structures?

Response: Please see our response to reviewer's comment #6.

14. Page 10, bottom left and elsewhere. Can you replace all instances of "largely agrees with" with something more quantitative – like backbone RMSD.

Response: Please see our response to reviewer's comment #6.

15. Page 11, left hand column. In addition to the pi stacking interactions, I'm wondering what the hydroxyl on the tyrosines are doing – are they finding anything to hydrogen bond

to? What?

Response: Please see our response to reviewer's comment #6.

16. Page 11, 2nd sentence of the 2nd paragraph: as for 14 above, please replace "generally in good agreement" with something more precise.

Response: Please see our response to reviewer's comment #6.

17. Page 11 – How do the starting and final structures and hydrophobic core compare to the experimental structure for Mini-B in SDS micelles?

Response: Please see our response to reviewer's comment #6.

18. Page 14 – right hand side, please replace "good overlap" and "remarkably analogous" with something more precise like RMSD.

Response: Please see our response to reviewer's comment #6.

Competing Interests: No competing interests were disclosed.